London Road, Bracknell
Berkshire RG12 2SZ

LONDON, METEOROLOGICAL OFFICE.
Met.O.11 Technical Note No.258

# Trials of the interactive radiation scheme in the global model.

287



MET O 11 TECHNICAL NOTE NO 258

# TRIALS OF THE INTERACTIVE RADIATION SCHEME IN THE GLOBAL MODEL

M. D. Gange

Met O 11 (Forecasting Research)

Meteorological Office

London Road

Bracknell

Berkshire

England

May 1987

## INTRODUCTION

This note presents the results of a series of test runs of the interactive radiation scheme in the Meteorological Office global model described by Dickinson (1984). The scheme is that which has been already included in the operational fine-mesh model and the aim of the test was to examine its performance in the global model. The scheme was found to produce a number of undesirable features in the forecasts. Various modifications to the scheme were then tried, to remove these deficiencies and reduce the systematic errors in the forecasts.

## ASSESSMENT OF THE TEST FORECASTS

The method used to assess the test runs of the radiation scheme was to look at zonally-averaged temperature cross-sections. In the real atmosphere, such zonal averages would change only slowly over periods of several days, and any large deviations produced by the model forecast would indicate systematic temperature biases.

It was found that similar results were obtained from all the cases tested, allowing for the seasonal variation between the hemispheres; therefore the results of running only 1 case (data-time 00z 1st August 1985) are presented here. All the forecasts were run to 3 days.

The various changes made to the model for each forecast run are listed in Table 1. The motivation for making each change is described in the following section. A new physics package including an implicit treatment of the boundary layer and split final detrainment in the convection scheme, as well as interactive radiation were also under trial, so some forecast runs included these changes.

The results of each of the 16 runs are shown in Figs. 1 - 15 in the form of zonally-averaged cross-sections of ('3-day forecast' - 'initial') temperatures. Figs. 16 - 25 show the differences between selected runs, this highlights the effects of individual changes.

## DISCUSSION OF RESULTS

The first forecast-run shown in Fig.1 is simply the version used operationally, which has a climatological radiation scheme. This means that cloud amounts and heating and cooling rates are specified as fixed functions of latitude. No time or longitudinal variation is allowed.Any future version of the model would need to perform as well as, or better, than this standard version. It can be seen that, for most of the atmosphere, zonally-averaged temperature biases are less than 1°C. However, there are some significant cold-biases at lower levels, particularly at 700 mb, in middle and high latitudes.



Fig. 2a shows the results of the forecast which includes the interactive radiation scheme instead of the climatological radiation scheme. Cloud amounts are diagnosed from the model relative humidity and heating and cooling rates diagnosed from these. The most striking feature of this forecast is the extremely large cold bias above 100 mb, which is most marked in the polar regions of the northern hemisphere. In these regions of the atmosphere, ozone plays an important part in the temperature balance. The radiative effects of ozone were omitted from the original scheme for computational economy. For run 2b, these effects were included in the interactive radiation scheme. A data-set of mean ozone concentrations above 200 mb for August was used as shown in Table 2. From these values, the top levels of the model above 200 mb were set to fixed ozone mixing ratios interpolated from these values. The bottom levels were assumed to have an ozone mixing ratio of $1 \times 10^{-8}$ g/g.

The forecast with this extension to the short-wave part of the radiation scheme is shown in Fig. 2b. Compared with run 2a, there is a lot more heating near the top of the model (where the highest ozone concentrations are to be found). However, there is still a very large cold bias centred now at 70 mb. Investigation of the forecast, revealed that this effect was probably being caused by the model being too moist at stratospheric levels. Table 3 shows zonally-averaged humidity mixing ratios forecast by the model at 300 mb and above. The stratosphere is, in reality, very dry with a humidity mixing ratio of $3 \times 10^{-6}$g/g being a typical climatological value. (Harries, 1976). The values shown by Table 3 are greatly in excess of this climatological value, particularly in the polar regions of the Northern Hemisphere.

The next alteration made to the forecast model was to 'impose' a more appropriate humidity structure at its upper levels. It was possible to change the humidities with respect only to the radiation calculations, i.e. the humidities used by the rest of the model physics and dynamics would be the same as in previous runs. In all, 5 different humidity structures were tried ( see Table 1). For H = 1 to 4, the humidity mixing ratio was adjusted so as to taper off to very low values at the top of the model. For H=5, the humidity mixing ratio was simply set to $3 \times 10^{-6}$ g/g in the whole of the stratosphere at the start of the forecast. The tropopause is located by the first level above 500 mb at which the lapse rate is less than 0.002 K /m. In the case of H = 5, the new humidity distribution was used for all calculations in the model. This humidity structure was the most realistic one used in the runs.

In run 3, the humidity of the model was adjusted down to level 7 ( $\simeq$ 590 mb). Fig.3 shows that this brought about a big reduction in the cold bias present in run 2b at 70 mb. On the other hand, cold biases became larger at levels between the 'imposed' humidity structure and the unadjusted lower levels of the model. In run 4, the humidity mixing ratio only in the top 4 levels of the model was changed. This forecast is also much better above 100 mb and in addition, has not become any worse between 600 and 850 mb. The runs including H=3 were noticeably warmer at around 200 mb. This is probably because of a much smaller vertical gradient of humidity mixing ratio, with this particular moisture structure, combined with large amounts of high-cloud diagnosed at this level.



All 5 imposed humidity structures were successful to a greater or lesser degree in reducing the cold bias in the stratosphere, but in each case, there remains a smaller cold bias of the order of 1 - 2°C around 70 mb. In order to try to eliminate this bias, the long-wave part of the radiation scheme was next modified to include the effects of ozone. As in the case of the short-wave part of the scheme, this change should again have maximum effect in the stratosphere, and as can be seen from Fig. 5, the temperature forecast is much improved here. The differences between runs 5 and 4 (see Fig. 17) show that the inclusion of the effect of ozone in the long-wave part has maximum impact around 70 mb.

The next aspect of the radiation scheme to be examined, was the cloud amounts diagnosed from the relative humidity. The formula used for calculating cloud amounts is

$$C_{H,M,L} = [(R - R_c)/(1 - R_c)]^2 \quad \text{for} \quad R > R_c$$

$$= 0 \quad \text{for } R < R_c \text{ or } R = R_c$$

where R is relative humidity, $R_c$ is threshold value of relative humidity for predicting cloud. In the original Met.O. 11 version of the scheme, $R_c$ = 85 %.

Table 4 shows zonally-averaged diagnosed cloud-amounts for 3 runs (numbers 7,8, and 15) of the model and also shows climatological cloud amounts for July (as used in the Met.O. 20 climate model (Slingo,1986)). The 3 forecasts have different values of $R_c$. The run with $R_c$ = 85, shows that

diagnosed cloud amounts are excessive, particularly at low and high cloud levels. The run with $R_c$ = 99 brings the cloud amounts much closer to climatological values, although amounts are still excessive in many places. The run with $R_c$ = 90 also includes some modifications to the model's convection scheme, in the form of split final detrainment (Slingo 1985) and also has a different boundary layer scheme (run 15 in Table 1). (These changes have removed the excessive relative humidity and have resulted in a better cloud simulation with a lower threshold than the $R_c$ = 99 run). Fig. 19 shows the effect on the temperature forecast of increasing $R_c$ from 85 to 99. It seems likely that reduced cloud amounts have allowed more solar radiation through to heat the lower layers, whilst at high-cloud levels, cooling has been brought about by more infra-red radiation being lost to space. Comparing Figs. 7 and 8, the version with $R_c$ = 99 produces a slightly better forecast.

Run 7 shows the result of changing the emissivity of high clouds from 0.75 to 0.5. Compared with run 6, the warm bias at 200 mb is reduced. The difference between runs 7 and 6 is shown by Fig. 18.

The original version of the radiation scheme diagnoses low cloud at model levels 2 - 4, medium at 5 - 7, and high at levels 8 - 12. In the operational model, level 11 is approximately 250 mb (≃ 34000 ft.) and level 12 is approximately 190 mb (≃ 40000 ft.). In the atmosphere, it is unusual for high layer cloud to be reported at these levels, outside the tropics. In run 9, diagnosed high cloud is restricted to levels 8 - 10. With this change, the warm bias at 200 mb present in run 7, disappears completely.



Fig.20 shows the difference between these two runs. The large differences at 200 mb in the tropics suggest that large amounts of cloud are being diagnosed by the model in these regions at levels 1 and 12, but part of the warm bias may also be due to the imposed humidity structure (H=3) of run 7.

With the original version of the interactive radiation scheme, difficulties arise because of the level at which the cloud-top cooling is inserted. Because the model-layers are thick, the insertion of the cooling at either the level of the cloud or the level above gives unrealistic results. However, the scheme was altered so that the maximum cooling would be shifted from the level above the cloud to the level containing the cloud. Runs 10 and 11 show the result of this change. The difference between these two runs, shown by Fig. 22, demonstrates clearly how the height of maximum cooling has been shifted downwards.

In the remaining four model runs (12 - 15), the operational boundary layer scheme has been replaced by an implicit boundary layer scheme (Kitchen 1986, Wilson 1987).The main impact of this new boundary layer scheme is to produce a slightly drier and colder boundary layer.

The original version of the radiation scheme only absorbs <u>downward</u> solar radiation. In run 14, the absorption of upward solar radiation (reflected from the surface and from clouds) was included. Comparing with run 13, there is little effect on the temperature in the troposphere. Fig. 24 shows the difference between the two runs. The large amount of extra

heating in the stratosphere is due to absorption by ozone of reflected solar radiation. The calculations involved in including this extra absorption, added about 50% to the cost of running the radiation scheme, whilst at the same time, only slightly improving the forecast.

The final run, run 15, had two modifications.

i) The convection scheme was modified to include the effect of split final detrainment.

ii) The constant $R_c$, described earlier, was changed to 90 % for levels 3 to 12 and to 95 % for level 2.

As was previously mentioned, this run produced more realistic cloud amounts and by comparing it with run 13, some improvement in temperatures at 850 mb can be seen. Fig. 25 shows the difference between run 15 and run 13.

## CONCLUSIONS

i) In terms of temperature biases, the forecast with the interactive radiation scheme was not as good as the forecast with the climatological radiation scheme, even when all the modifications beneficial to the interactive scheme were included.

ii) The performance of the interactive radiation scheme is strongly dependent on the forecast humidity structure of the model. This in turn



depends greatly on the realistic parametrization of all the other physical processes in the model. Further improvement in the performance of the radiation scheme is unlikely without improvements to the representation of these processes.

In view of the above , it is recommended that the operational coarse-mesh model should continue to use the climatological radiation scheme at the present time.

TABLE 1 List of Test Forecasts
(see below for explanation of abbreviations.)

| Run | H | $C_L$ | $C_M$ | $C_H$ | $R_C$ | CCL | $\epsilon_H$ | IBL | $O_3$ | RSB | SFD | RAD |
|---|---|---|---|---|---|---|---|---|---|---|---|---|
| 1 | | | | | | | | | | | | C |
| 2a | | 2-4 | 5-7 | 8-12 | 85 | | | | | | | I |
| 2b | | 2-4 | 5-7 | 8-12 | 85 | | | | S | | | I |
| 3 | 1 | 2-4 | 5-7 | 8-12 | 85 | | | | S | | | I |
| 4 | 2 | 2-4 | 5-9 | 10-12 | 99 | * | | | S | | | I |
| 5 | 2 | 2-4 | 5-9 | 10-12 | 99 | * | | | LS | | | I |
| 6 | 3 | 2-4 | 5-7 | 8-12 | 99 | * | | | LS | | | I |
| 7 | 3 | 2-4 | 5-7 | 8-12 | 99 | * | .5 | | LS | | | I |
| 8 | 3 | 2-4 | 5-7 | 8-12 | 85 | * | .5 | | LS | | | I |
| 9 | 3 | 2-4 | 5-7 | 8-10 | 99 | * | .5 | | LS | | | I |
| 10 | 5 | 2-4 | 5-7 | 8-11 | 85 | | | | LS | | | I |
| 11 | 5 | 2-4 | 5-7 | 8-11 | 85 | * | | | LS | | | I |
| 12 | 4 | 2-4 | 5-9 | 10-12 | 85 | * | | * | S | | | I |
| 13 | 5 | 2-4 | 5-9 | 10-12 | 85 | * | | * | LS | | | I |
| 14 | 5 | 2-4 | 5-9 | 10-12 | 85 | * | | * | LS | * | | I |
| 15 | 5 | 2-4 | 5-9 | 10-12 | 90† | * | | * | LS | | * | I |

†95 for low cloud at level 2.

H Indicates modifications were made to the humidity structure for this run. ( $R_i$ indicates relative humidity modified at model-level i) ( $r_i$ indicates humidity mixing ratio modified at model-level i)

H = 1 : $r_{13}^*, r_{12}^*, r_{11}^* = 3 \times 10^{-6}$ g/g, $R_{10}^* = 25\%$, $R_9^* = 25\%$, $R_8^* = 35\%$, $R_7^* = 45\%$ .

H = 2 : $r_{15}^* = 0.2 \times r_{14}$, $r_{14}^* = 0.4 \times r_{14}$, $r_{13}^* = 0.6 \times r_{13}$, $r_{12}^* = 0.8 \times r_{12}$ .



H = 3 : $r_{15}^* = 0.13 \times r_{11}$, $r_{14}^* = 0.26 \times r_{11}$, $r_{13} = 0.5 \times r_{11}$, $r_{12} = 0.76 \times r_{11}$ .

H = 4 : $r_{15}^*, r_{14}^*, r_{13}^* = 3 \times 10^{-6}$ g/g, $r_{12}^* = \frac{1}{2}(r_{12} + 3\times10^{-6})$ g/Kg.

H = 5 : Stratospheric humidity mixing ratio set to $3 \times 10^{-6}$ g/g at start of forecast.

$C_L$ Model levels used for calculating low cloud.

$C_M$ Model levels used for calculating medium-level cloud.

$C_H$ Model levels for calculating high cloud.

$R_C$ Value of relative humidity threshold used in formula for diagnosing cloud amounts.

$$C_{H,M,L} = [(R - R_C)/(1 - R_C)]^2 \quad \text{for} \quad R > R_C$$
$$= 0 \qquad\qquad\qquad\qquad R < R_C$$

CCL Model-level at which cloud-top cooling is inserted. (*) indicates maximum cooling at level within cloud, otherwise maximum cooling at level above cloud.

$\epsilon_H$ Emissivity of high-cloud. If not specified, a default value of 0.75 was used.

IBL Implicit boundary layer included in the run.

$O_3$ Effects of ozone included in the forecast. (S) = ozone in short-wave part of radiation scheme, (L) = ozone in long-wave part of radiation scheme.

RSB Absorption of reflected solar radiation included.

SFD Split final detrainment included in convection scheme.

RAD (C) = climatological radiation scheme. (I) = interactive radiation scheme.

TABLE 2 Ozone Concentrations used in Forecasts (μg/g)

| Latitude | Pressure Level (mb) 100 - 200 | 120 - 160 | 80 - 120 | 40 - 80 | 0 - 40 |
|---|---|---|---|---|---|
| 81 N | 0.8 | 1.2 | 2.1 | 3.6 | 4.6 |
| 72 N | 0.7 | 1.1 | 1.9 | 3.7 | 5.1 |
| 63 N | 0.7 | 1.0 | 1.8 | 3.7 | 5.9 |
| 54 N | 0.5 | 0.8 | 1.6 | 3.5 | 6.6 |
| 45 N | 0.4 | 0.6 | 1.2 | 3.2 | 7.3 |
| 36 N | 0.3 | 0.4 | 0.8 | 2.8 | 7.8 |
| 27 N | 0.3 | 0.4 | 0.6 | 2.4 | 8.1 |
| 18 N | 0.1 | 0.2 | 0.5 | 2.0 | 8.5 |
| 9 N | 0.1 | 0.1 | 0.4 | 1.8 | 8.9 |
| 0 | 0.1 | 0.1 | 0.3 | 1.6 | 9.2 |
| 9 S | 0.1 | 0.1 | 0.3 | 1.7 | 9.6 |
| 18 S | 0.1 | 0.1 | 0.4 | 2.0 | 9.7 |
| 27 S | 0.2 | 0.3 | 0.6 | 2.6 | 9.2 |
| 36 S | 0.4 | 0.6 | 1.1 | 3.5 | 8.3 |
| 45 S | 0.5 | 0.8 | 1.5 | 3.9 | 7.6 |
| 54 S | 0.7 | 1.2 | 2.0 | 4.1 | 6.7 |
| 63 S | 0.9 | 1.4 | 2.3 | 4.1 | 5.7 |
| 72 S | 1.0 | 1.5 | 2.4 | 3.9 | 5.0 |
| 81 S | 1.0 | 1.6 | 2.3 | 3.7 | 4.7 |



TABLE 3 3-day Forecast Humidity Mixing Ratios (g/g) × $10^3$

| Latitude | Pressure Level (mb) 70 | 100 | 200 | 300 |
|---|---|---|---|---|
| 81 N | 135 | 139 | 116 | 89 |
| 72 N | 180 | 162 | 115 | 105 |
| 63 N | 114 | 124 | 94 | 121 |
| 54 N | 70 | 66 | 67 | 146 |
| 45 N | 44 | 33 | 57 | 270 |
| 36 N | 22 | 15 | 50 | 268 |
| 27 N | 16 | 9 | 48 | 336 |
| 18 N | 16 | 9 | 53 | 374 |
| 9 N | 17 | 9 | 45 | 338 |
| 0 | 17 | 8 | 43 | 288 |
| 9 S | 15 | 8 | 36 | 223 |
| 18 S | 15 | 8 | 30 | 159 |
| 27 S | 22 | 14 | 37 | 168 |
| 36 S | 31 | 27 | 35 | 90 |
| 45 S | 34 | 30 | 29 | 48 |
| 54 S | 24 | 22 | 15 | 28 |
| 63 S | 8 | 8 | 7 | 19 |
| 72 S | 3 | 3 | 4 | 10 |
| 81 S | 2 | 2 | 4 | 11 |

TABLE 4 Zonally-averaged Cloud Amounts (%) ( 3-day forecast) for various values of $R_c$

| Lat. | LOW | | | | MEDIUM | | | | HIGH | | | | CONVECTIVE | | | |
|---|---|---|---|---|---|---|---|---|---|---|---|---|---|---|---|---|
| | C | 85 | 99 | 90 | C | 85 | 99 | 90 | C | 85 | 99 | 90 | C | 85 | 99 | 90 |
| 81 N | 42 | 84 | 60 | 60 | 11 | 18 | 7 | 23 | 27 | 27 | 13 | 6 | 4 | 1 | 1 | 1 |
| 72 N | 45 | 71 | 42 | 45 | 13 | 32 | 20 | 36 | 29 | 41 | 22 | 15 | 5 | 4 | 2 | 4 |
| 63 N | 42 | 64 | 34 | 42 | 12 | 50 | 32 | 53 | 26 | 55 | 44 | 32 | 5 | 8 | 9 | 9 |
| 54 N | 40 | 55 | 31 | 33 | 10 | 34 | 19 | 34 | 21 | 43 | 32 | 31 | 5 | 8 | 8 | 9 |
| 45 N | 34 | 51 | 33 | 32 | 9 | 19 | 9 | 25 | 18 | 48 | 37 | 36 | 5 | 7 | 6 | 6 |
| 36 N | 25 | 48 | 36 | 24 | 7 | 8 | 5 | 13 | 14 | 32 | 27 | 28 | 4 | 7 | 7 | 6 |
| 27 N | 23 | 50 | 39 | 23 | 6 | 4 | 2 | 7 | 14 | 36 | 28 | 29 | 3 | 10 | 9 | 7 |
| 18 N | 26 | 52 | 33 | 22 | 7 | 8 | 4 | 11 | 19 | 43 | 33 | 34 | 4 | 11 | 11 | 9 |
| 9 N | 28 | 57 | 22 | 23 | 8 | 9 | 4 | 16 | 22 | 53 | 48 | 50 | 7 | 11 | 10 | 10 |
| 0 | 25 | 65 | 40 | 22 | 7 | 12 | 8 | 15 | 16 | 49 | 44 | 44 | 5 | 12 | 12 | 9 |
| 9 S | 24 | 68 | 48 | 25 | 6 | 6 | 5 | 6 | 11 | 34 | 28 | 23 | 4 | 15 | 14 | 11 |
| 18 S | 23 | 64 | 46 | 32 | 5 | 8 | 4 | 6 | 11 | 21 | 16 | 13 | 3 | 14 | 14 | 10 |
| 27 S | 27 | 61 | 46 | 31 | 5 | 14 | 7 | 17 | 12 | 36 | 29 | 25 | 4 | 13 | 13 | 11 |
| 36 S | 37 | 62 | 44 | 35 | 4 | 30 | 22 | 33 | 11 | 40 | 34 | 31 | 4 | 17 | 17 | 15 |
| 45 S | 44 | 77 | 60 | 58 | 5 | 45 | 36 | 47 | 12 | 41 | 33 | 26 | 5 | 21 | 21 | 18 |
| 54 S | 52 | 77 | 62 | 69 | 6 | 57 | 45 | 49 | 13 | 47 | 41 | 32 | 5 | 19 | 19 | 17 |
| 63 S | 50 | 83 | 72 | 70 | 7 | 53 | 44 | 58 | 13 | 59 | 54 | 48 | 5 | 14 | 13 | 12 |
| 72 S | 34 | 61 | 53 | 33 | 10 | 30 | 19 | 30 | 8 | 37 | 30 | 21 | 3 | 3 | 3 | 3 |
| 81 S | 21 | 80 | 65 | 62 | 12 | 70 | 55 | 73 | 5 | 74 | 62 | 28 | 2 | 1 | 0 | 1 |

C = Climatological cloud amounts

85 = $R_c$ set to 85 % (Run 7)

99 = $R_c$ set to 99 % (Run 8)

90 = $R_c$ set to 90 % (Run 15)



References


| | | |
|---|---|---|
| Dickinson A. | 1984 | Operational Numerical Weather Prediction System Documentation Paper No. 4 The Weather Prediction Model. |
| Harries, J.E. | 1976 | The distribution of water vapor in the stratosphere. Washington. Amer. Geoph. Union. Rev. Geoph. Space Phys. 14, 1976 pp. 565-575. |
| Kitchen, J.E. | 1986 | Met.O.11 Technical Note No.222. An implicit version of the operational model boundary layer routine. |
| Slingo, A. | 1985 | Handbook of the Meteorological Office 11-layer atmospheric general circulation model. Volume 1: Model Description. DCTN 29 Sept. 1985 p.127 |
| Slingo, A., Wilderspin, R.C. | 1986 | Development of a revised longwave radiation scheme for an atmospheric general circulation model. Bracknell: Royal Met.Soc. Q.J. 112:1986:No.472 pp.371-386. |
| Wilson, C.A. | 1987 | Met.O.11 Technical note-to be published. |

Fig. 1 ZONALLY-AVERAGED TEMPERATURES (3-DAY F/C - T+0) DT 0Z 1/8/85 : RUN 1

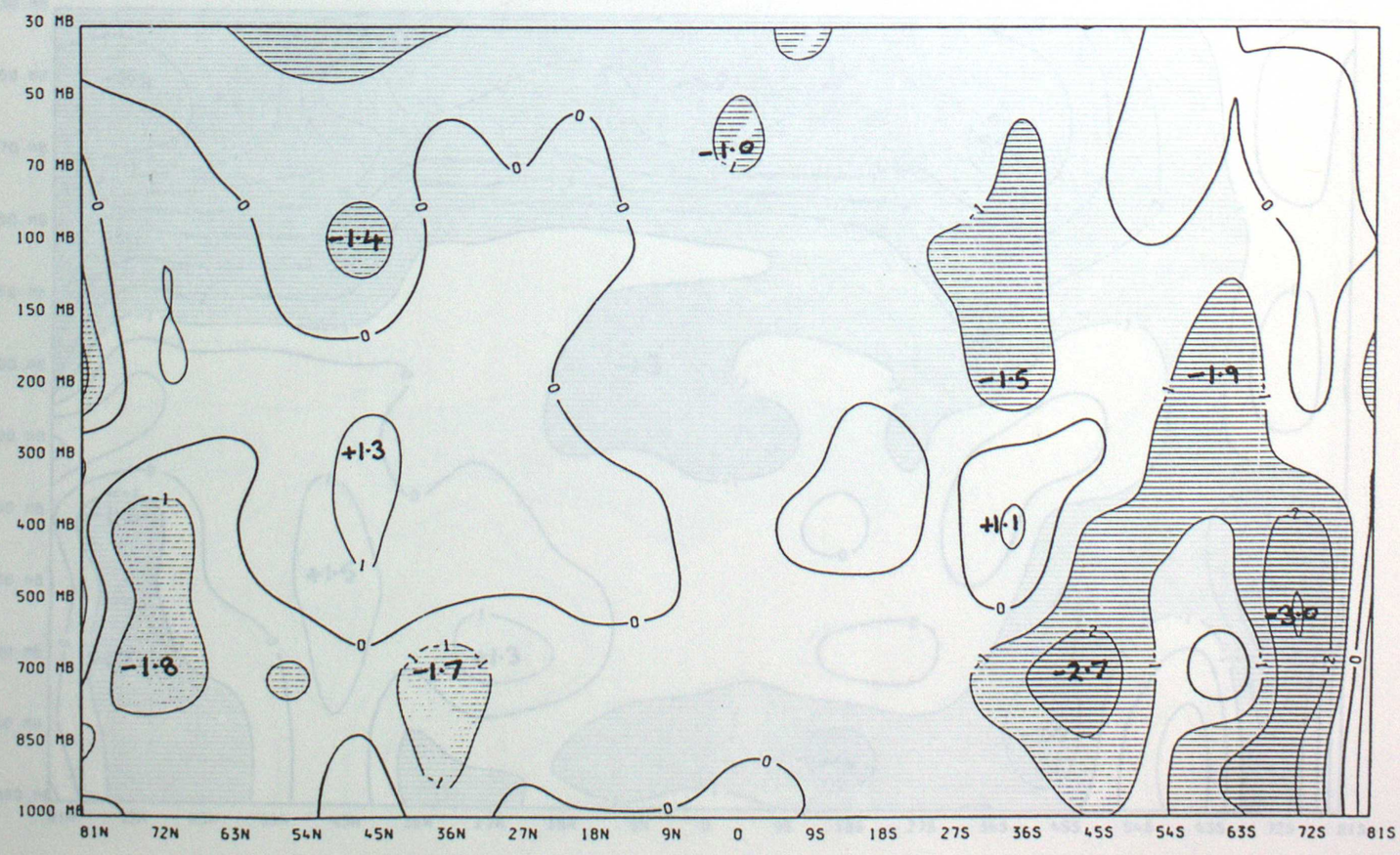

Fig. 2a ZONALLY-AVERAGED TEMPERATURES (3-DAY F/C - T+0) DT 0Z 1/8/85 : RUN 2A

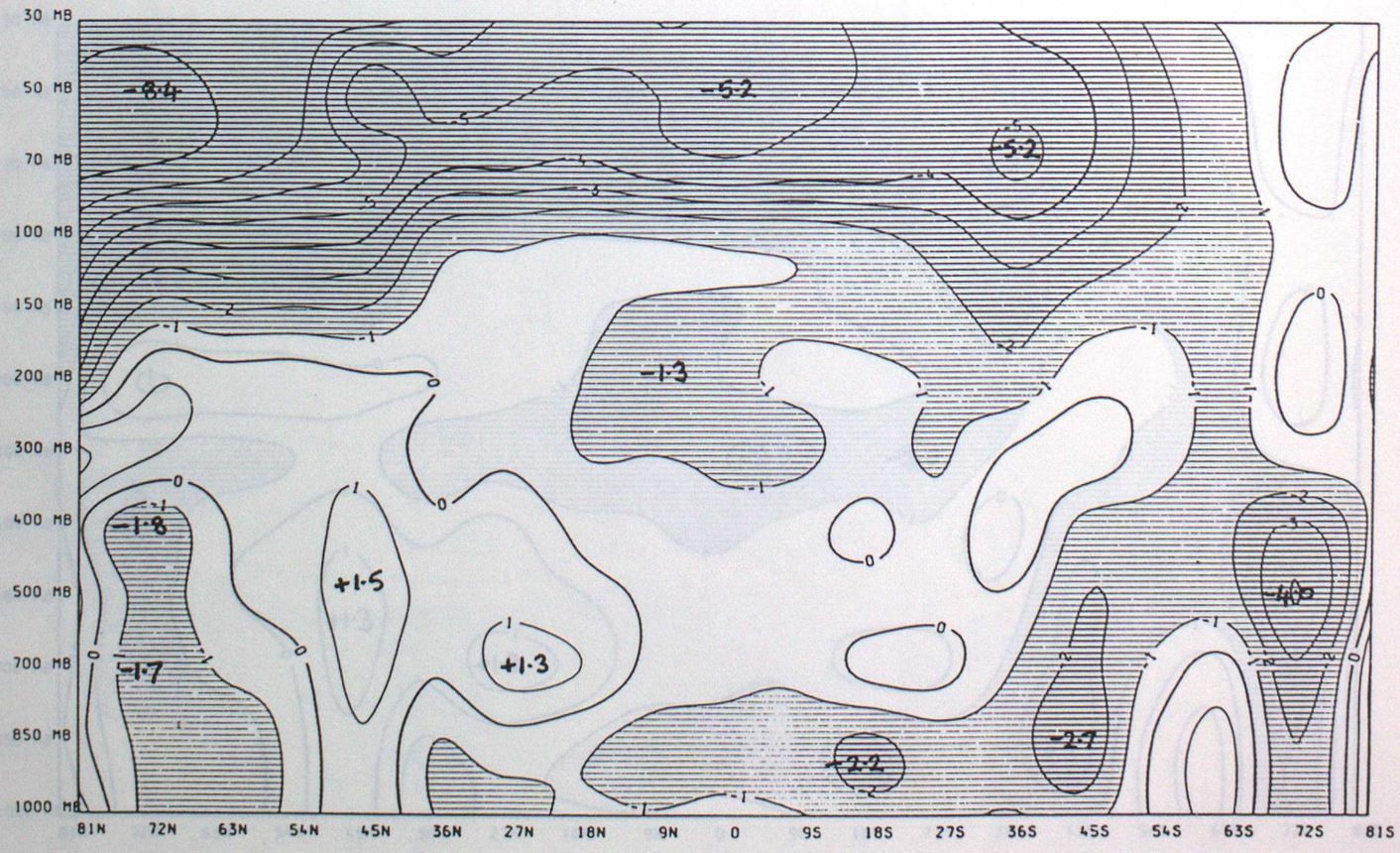

Fig. 2b ZONALLY-AVERAGED TEMPERATURES (3-DAY F/C - T+0) DT 0Z 1/8/85 : RUN 2B

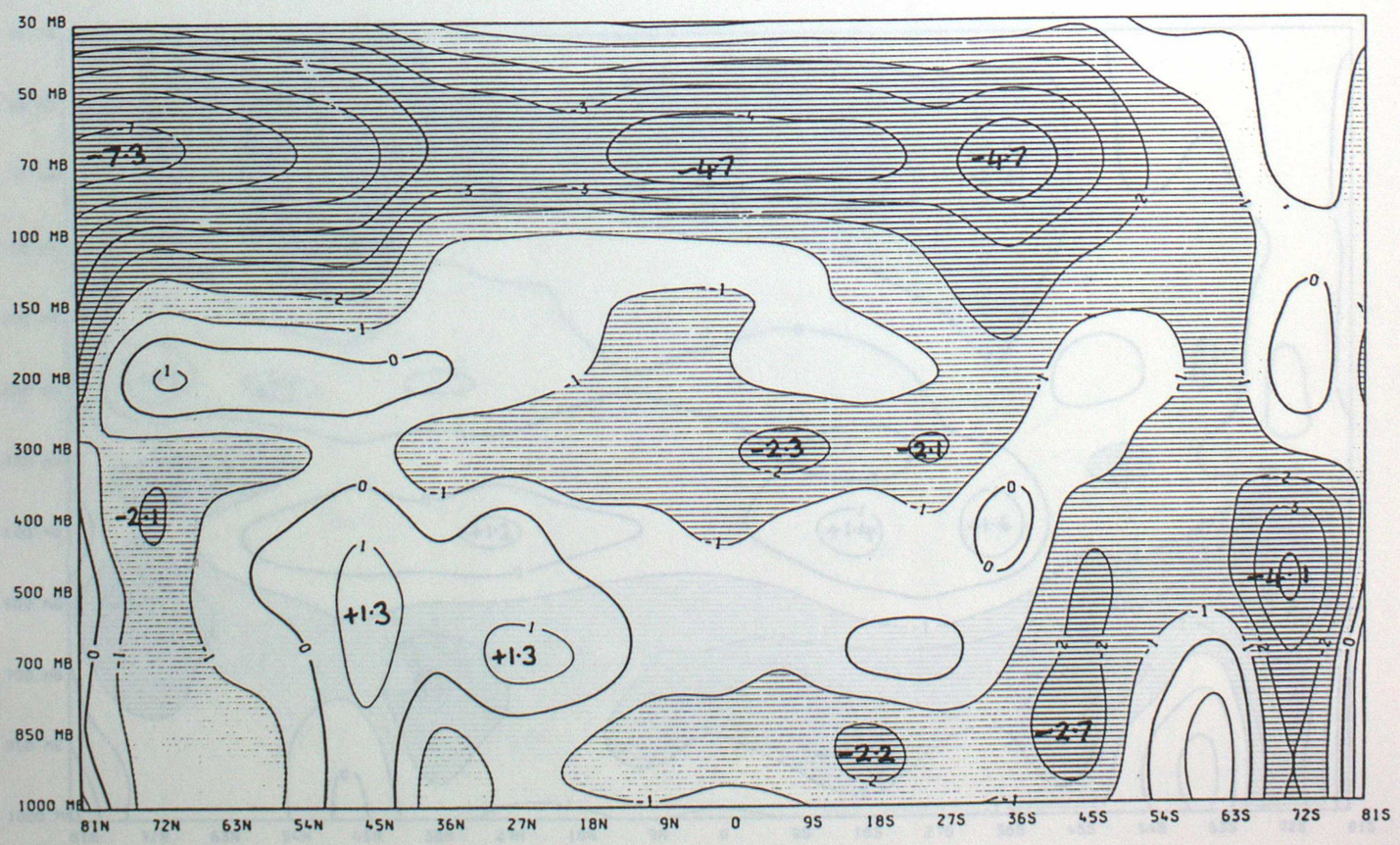

Fig.3 ZONALLY-AVERAGED TEMPERATURES (3-DAY F/C - T+0) DT 0Z 1/8/85 : RUN 3

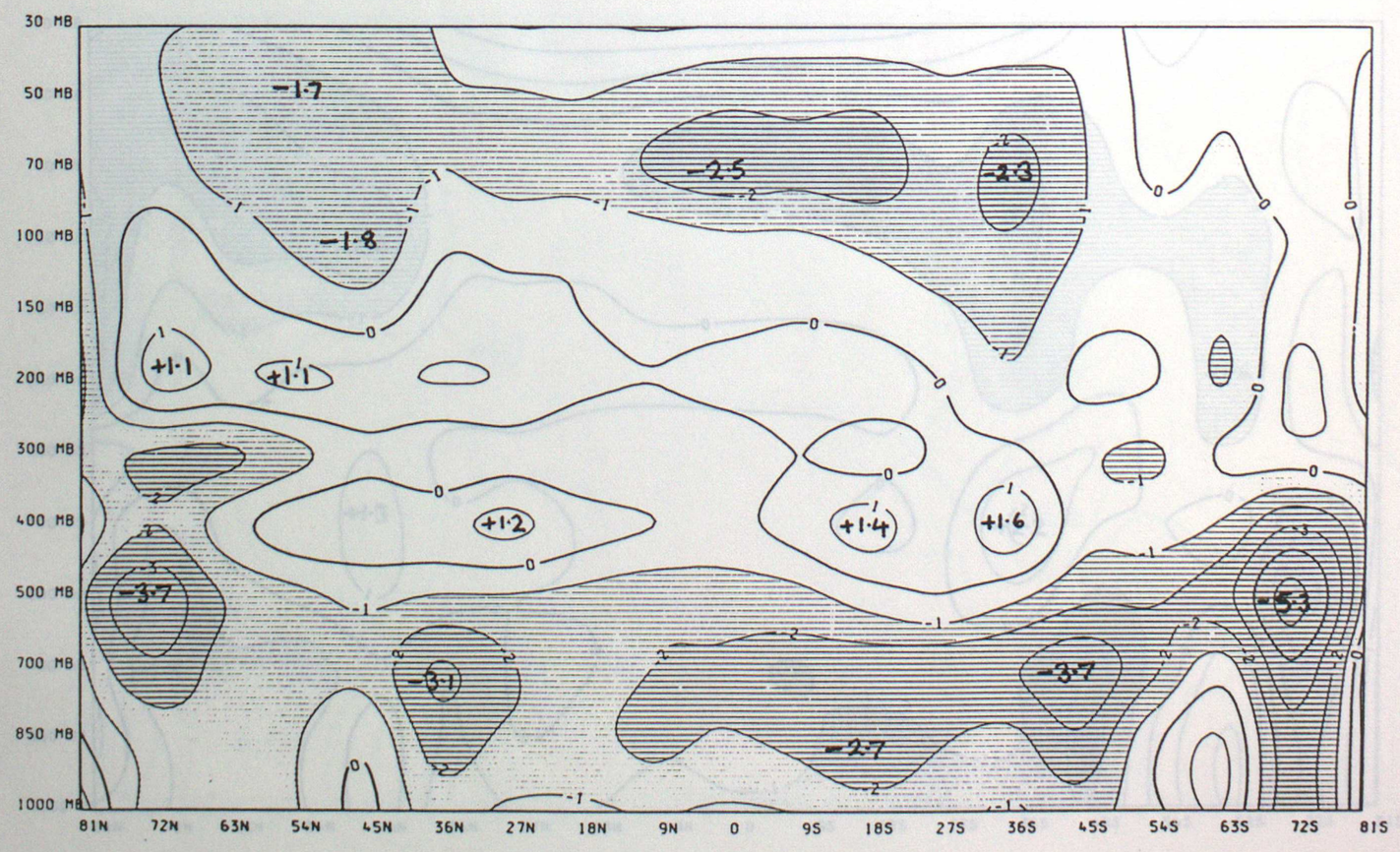

Fig.4 ZONALLY-AVERAGED TEMPERATURES (3-DAY F/C - T+0) DT 0Z 1/8/85 : RUN 4

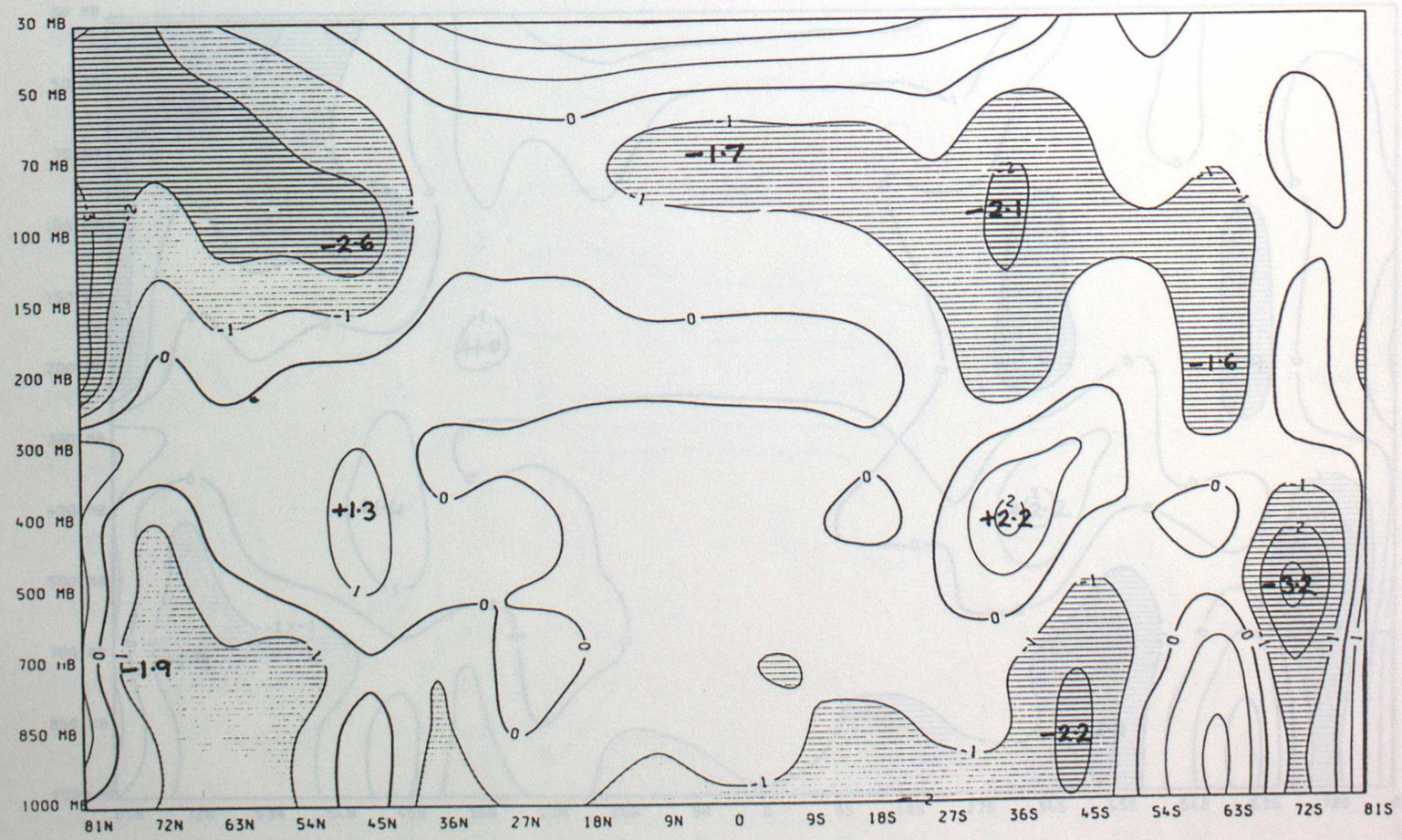

Fig. 5 ZONALLY-AVERAGED TEMPERATURES (3-DAY F/C - T+0) DT 0Z 1/8/85 : RUN 5

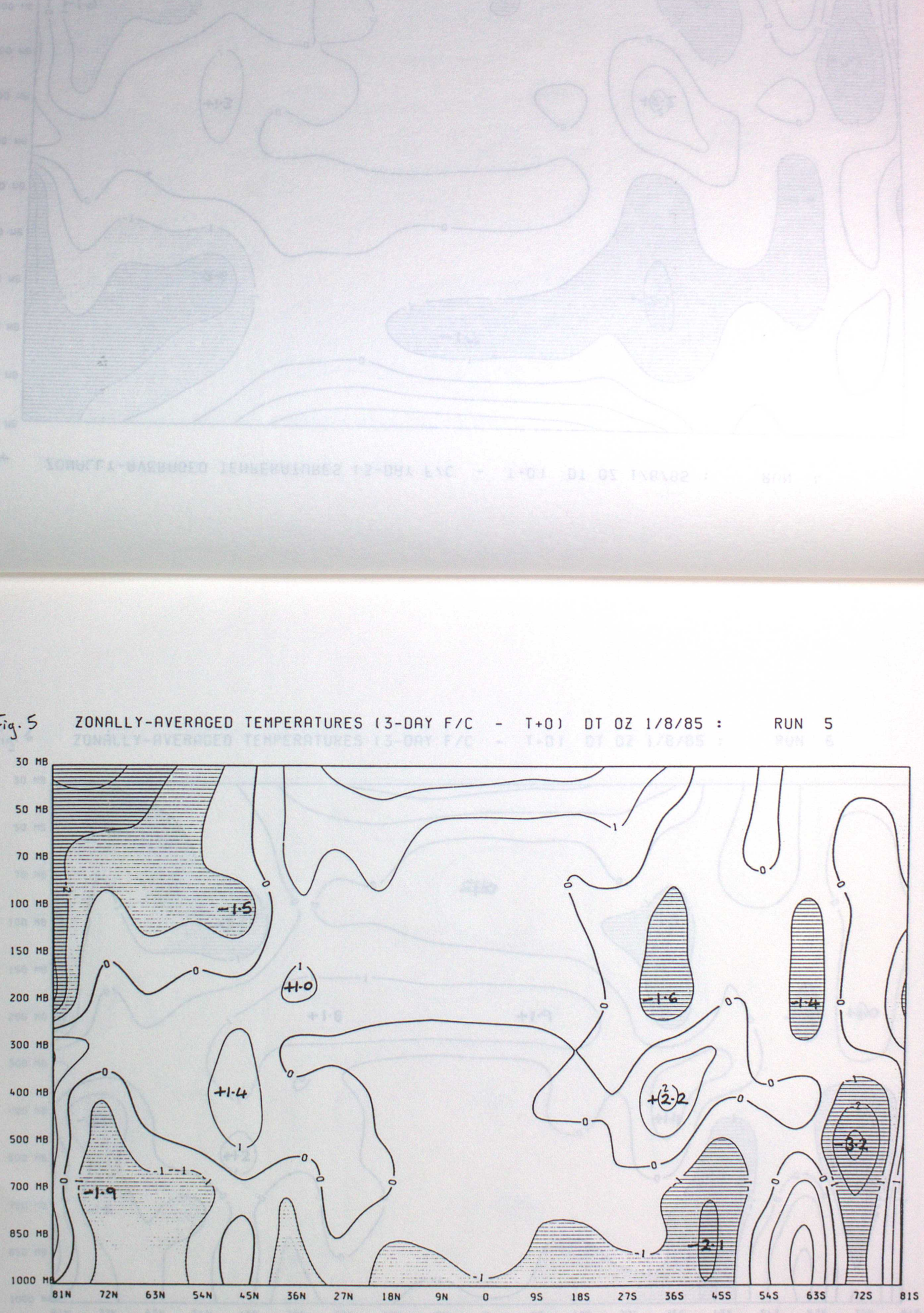

Fig. 6 ZONALLY-AVERAGED TEMPERATURES (3-DAY F/C - T+0) DT 02 1/8/85 : RUN 6

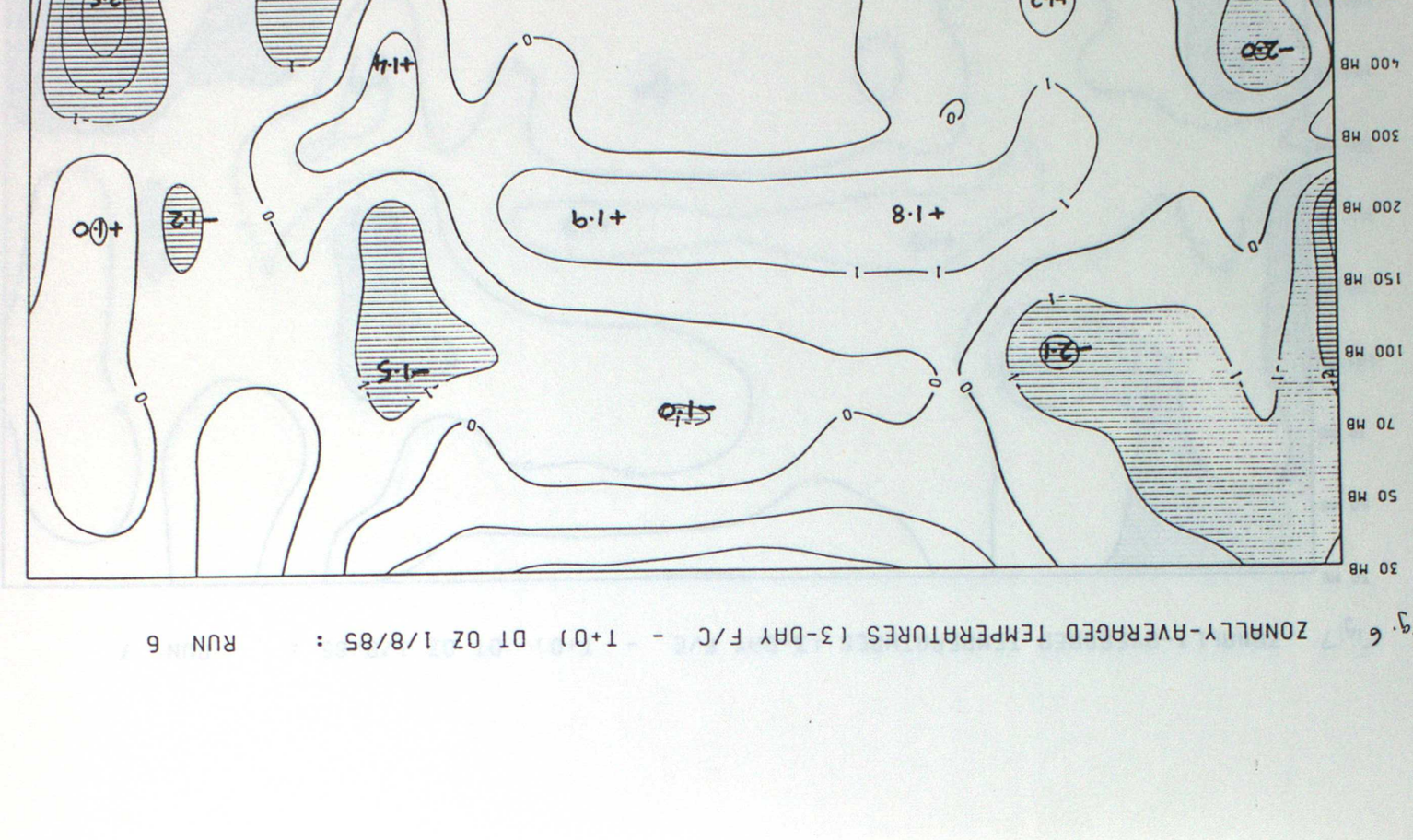

Fig.7 ZONALLY-AVERAGED TEMPERATURES (3-DAY F/C - T+0) DT OZ 1/8/85 : RUN 7

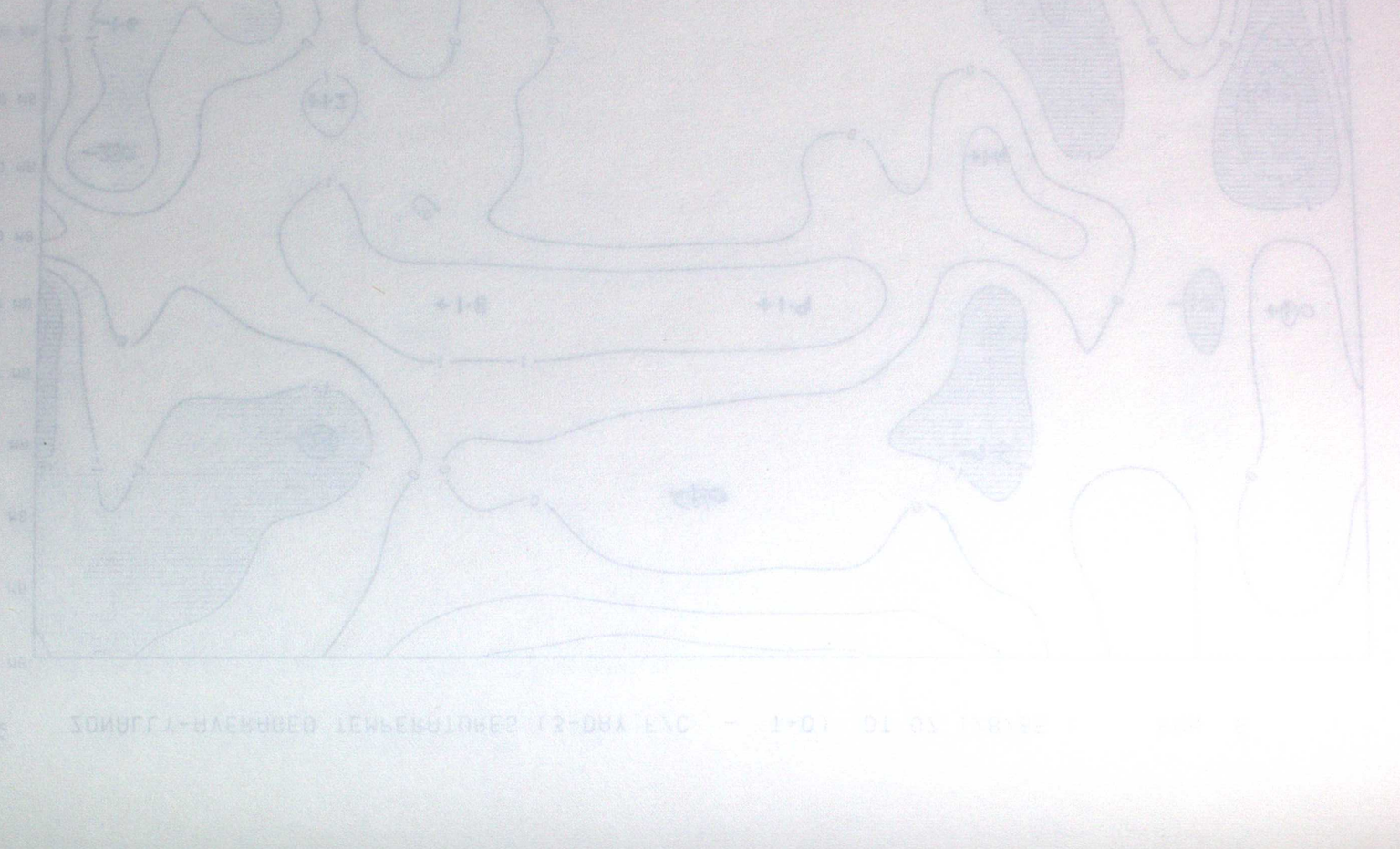

Fig.8 ZONALLY-AVERAGED TEMPERATURES (3-DAY F/C - T+0) DT 02 1/8/85 : RUN 8

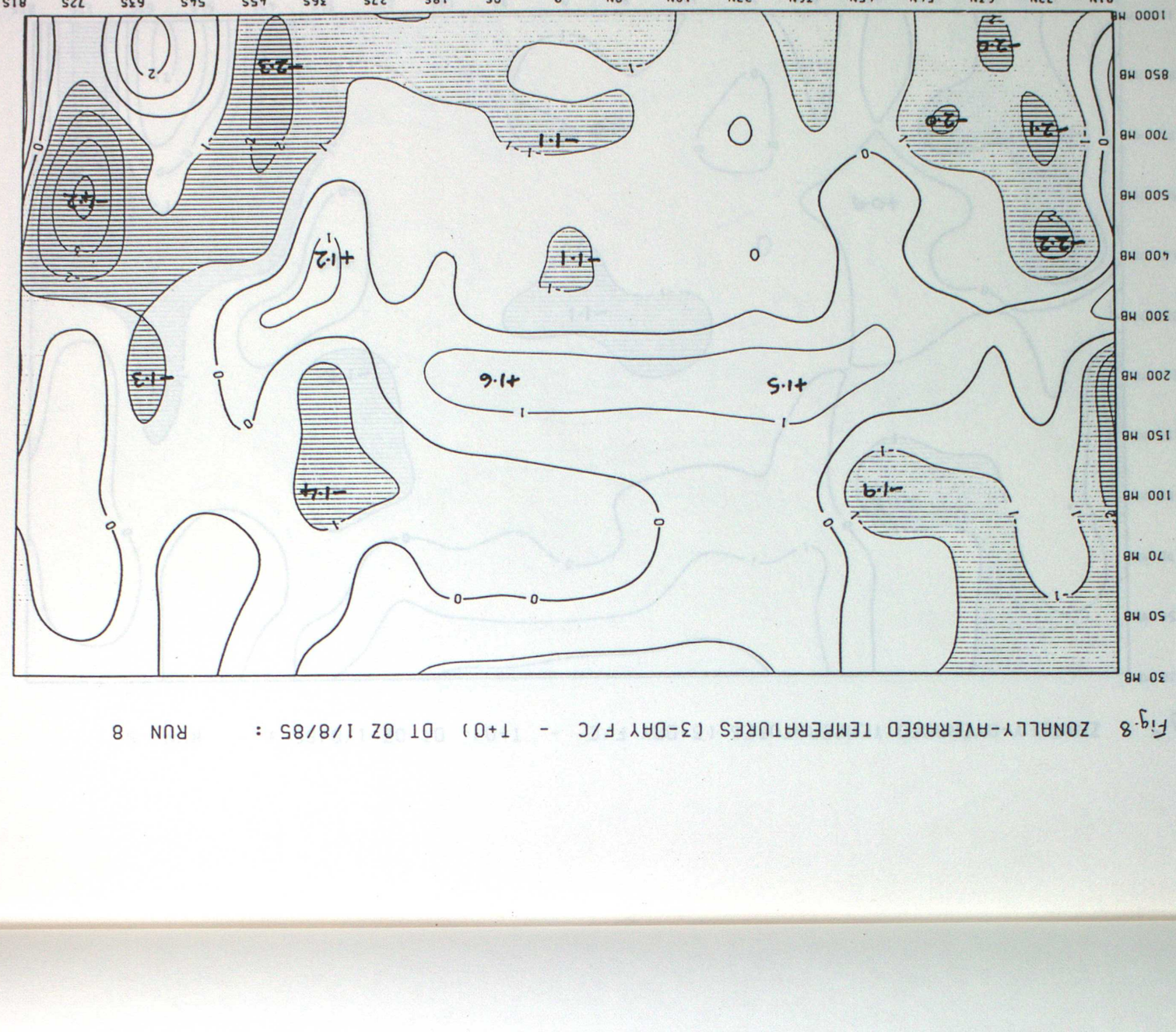

Fig.9 ZONALLY-AVERAGED TEMPERATURES (3-DAY F/C - T+0) DT OZ 1/8/85 : RUN 9

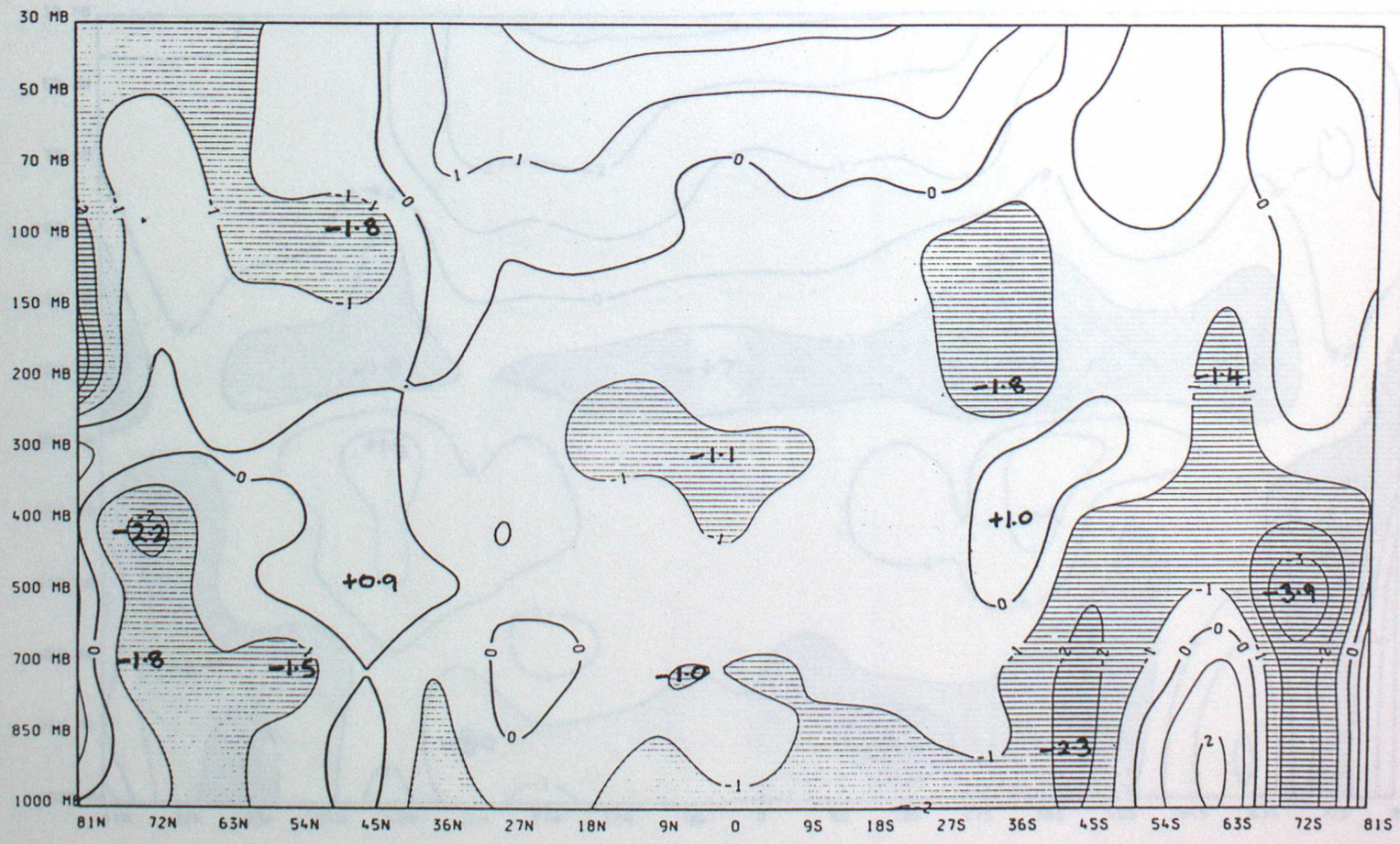

Fig. 10 ZONALLY-AVERAGED TEMPERATURES (3-DAY F/C - T+0) DT 0Z 1/8/85 : RUN 10

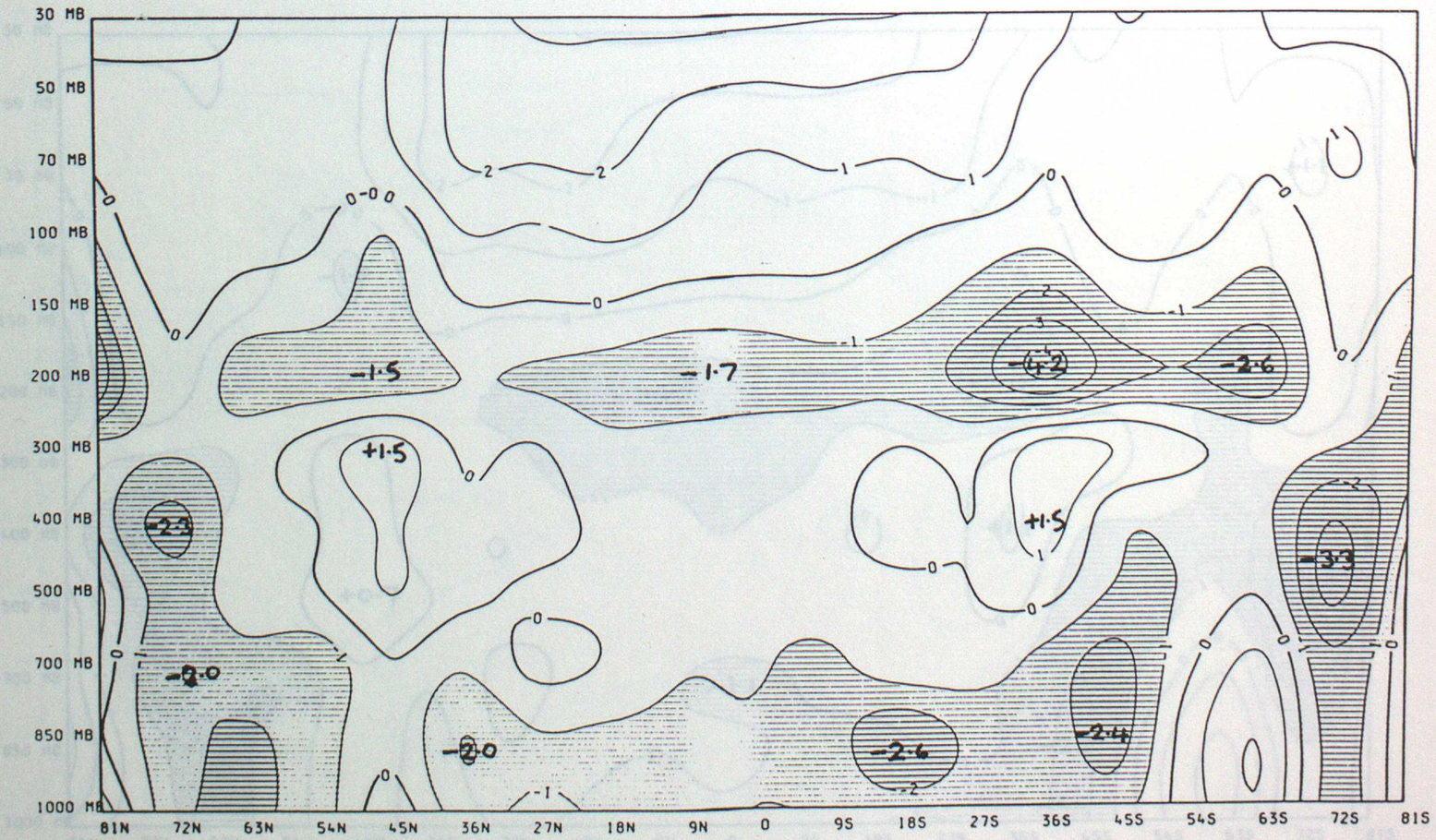

Fig. 11 ZONALLY-AVERAGED TEMPERATURES (3-DAY F/C - T+0) DT 0Z 1/8/85 : RUN 11

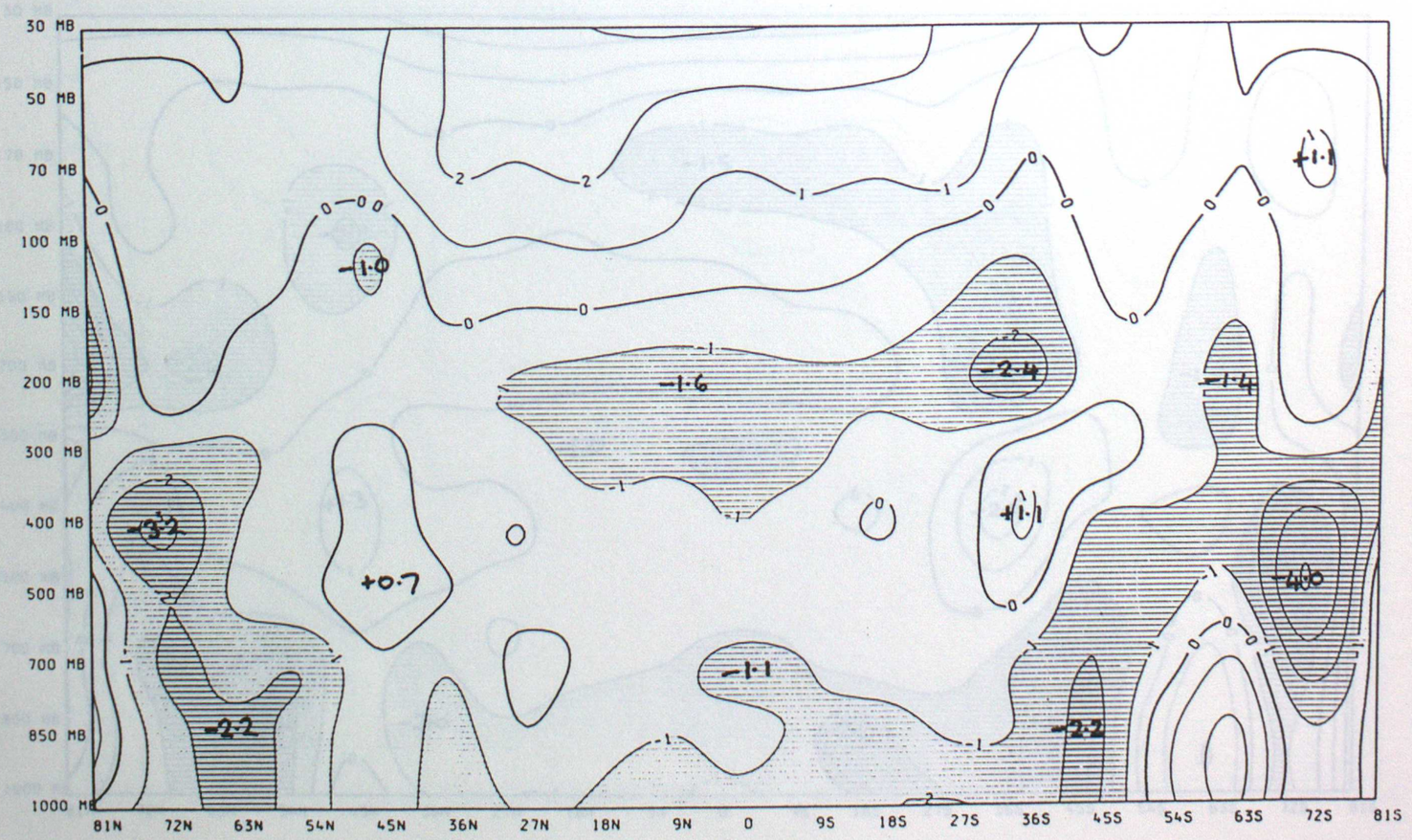

Fig. 12 ZONALLY-AVERAGED TEMPERATURES (3-DAY F/C - T+0) DT OZ 1/8/85 : RUN 12

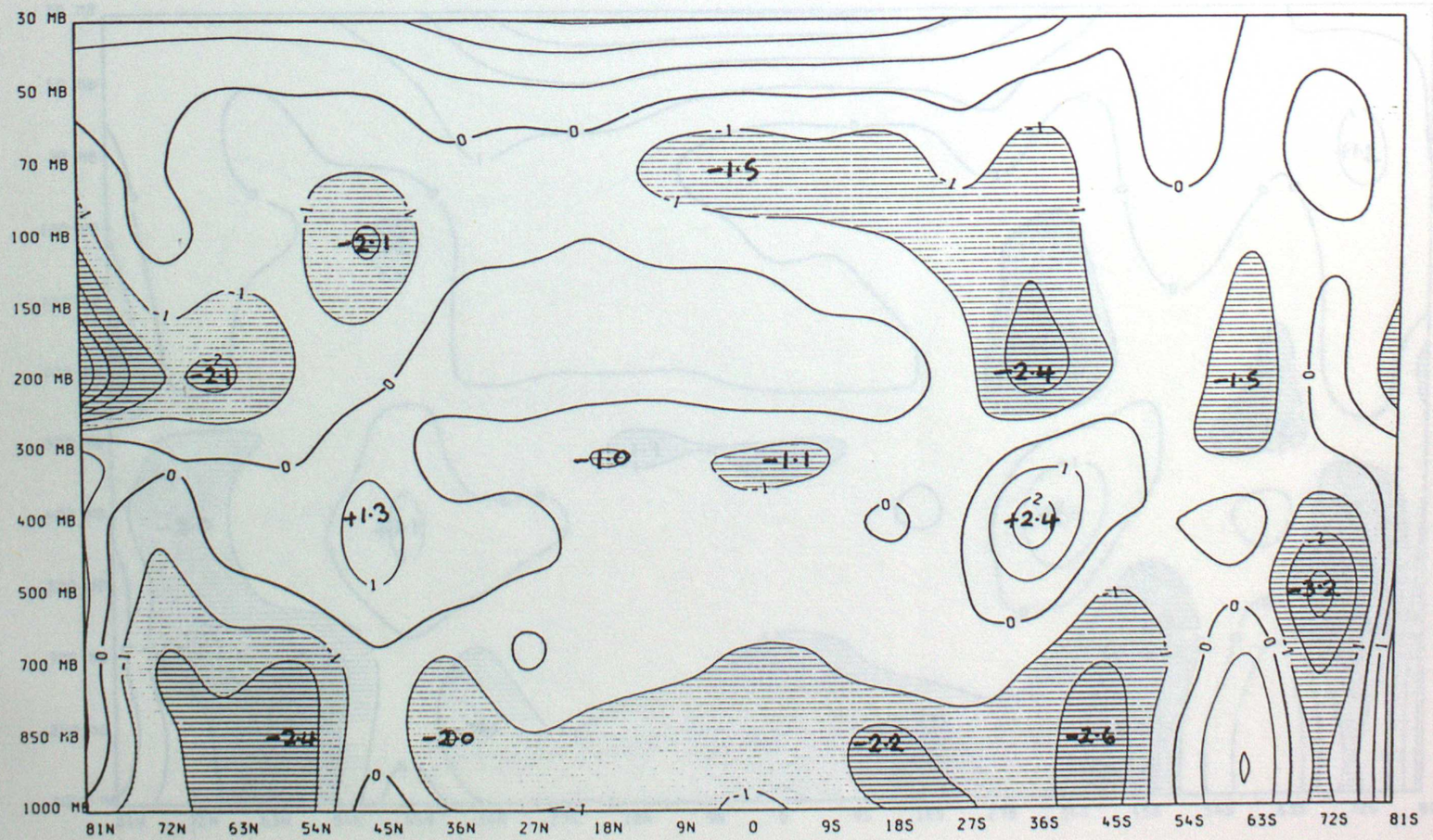

Fig. 13 ZONALLY-AVERAGED TEMPERATURES (3-DAY F/C - T+0) DT 0Z 1/8/85 : RUN 13

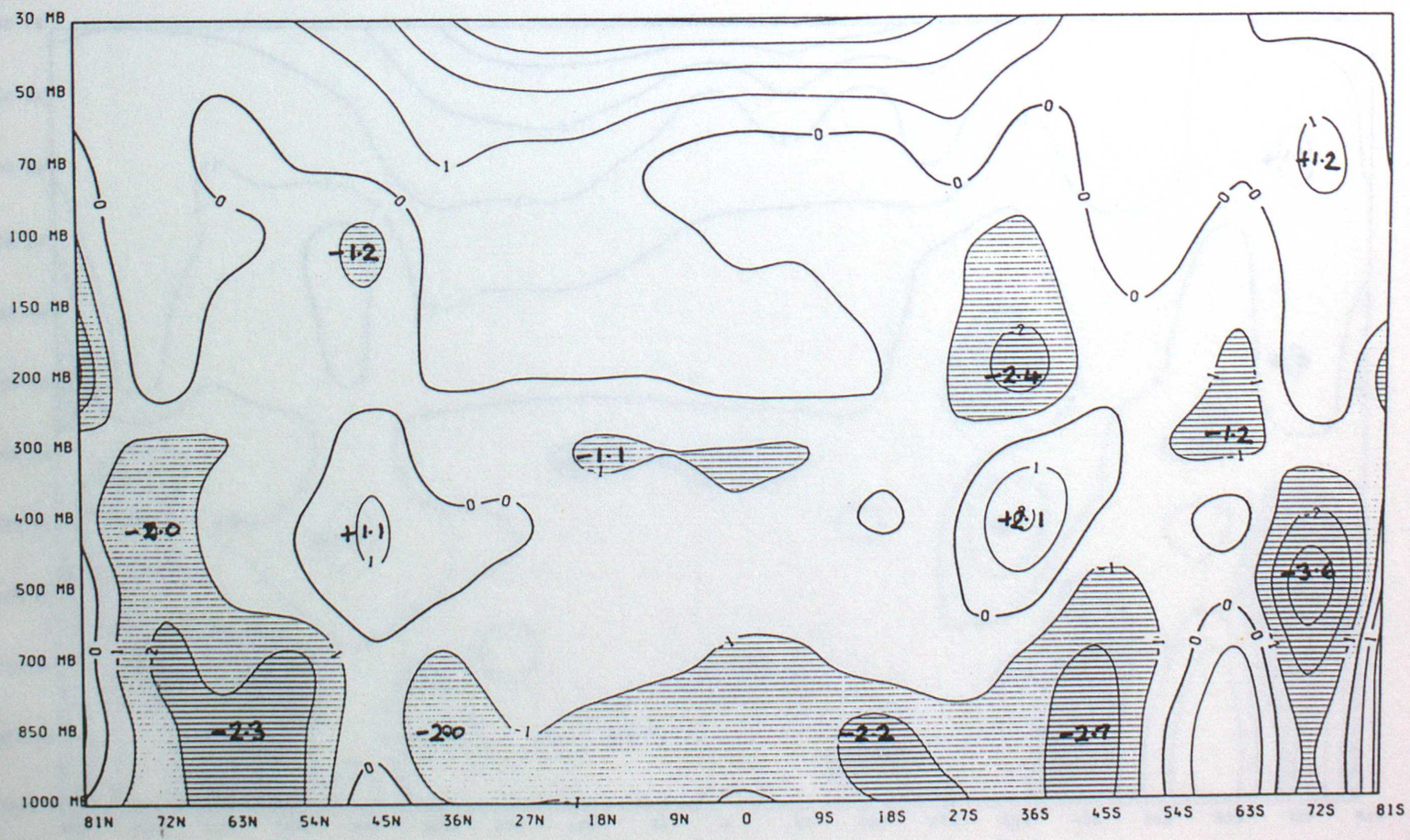

Fig. 14 ZONALLY-AVERAGED TEMPERATURES (3-DAY F/C - T+0) 0T 0Z 1/8/85 : RUN 14

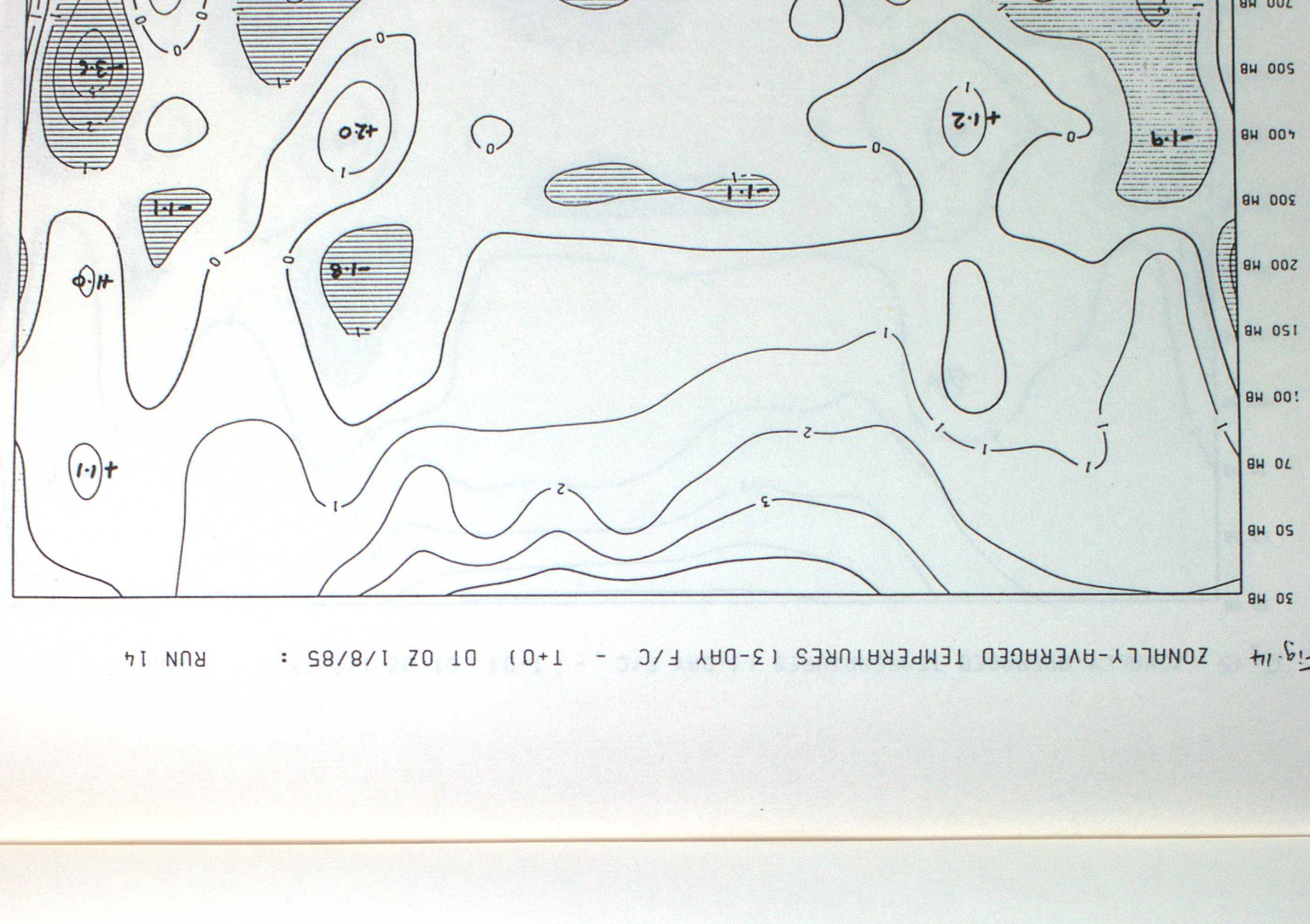

Fig.15 ZONALLY-AVERAGED TEMPERATURES (3-DAY F/C - T+0) DT 0Z 1/8/85 : RUN 15

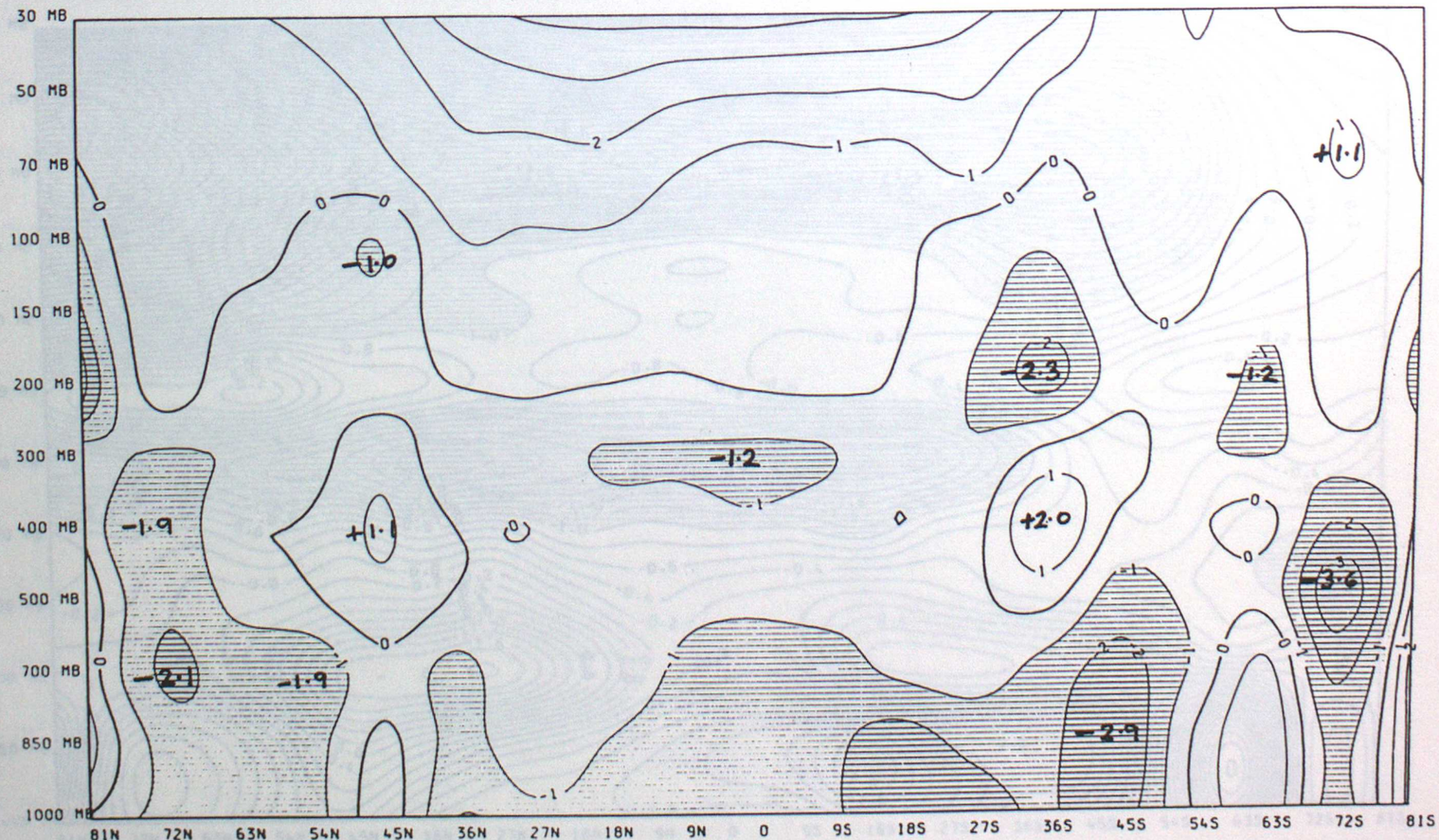

Fig.16 ZONALLY-AVERAGED TEMPERATURES (3-DAY F/C - T+0) DT 0Z 1/8/85 : RUN2B- RUN1

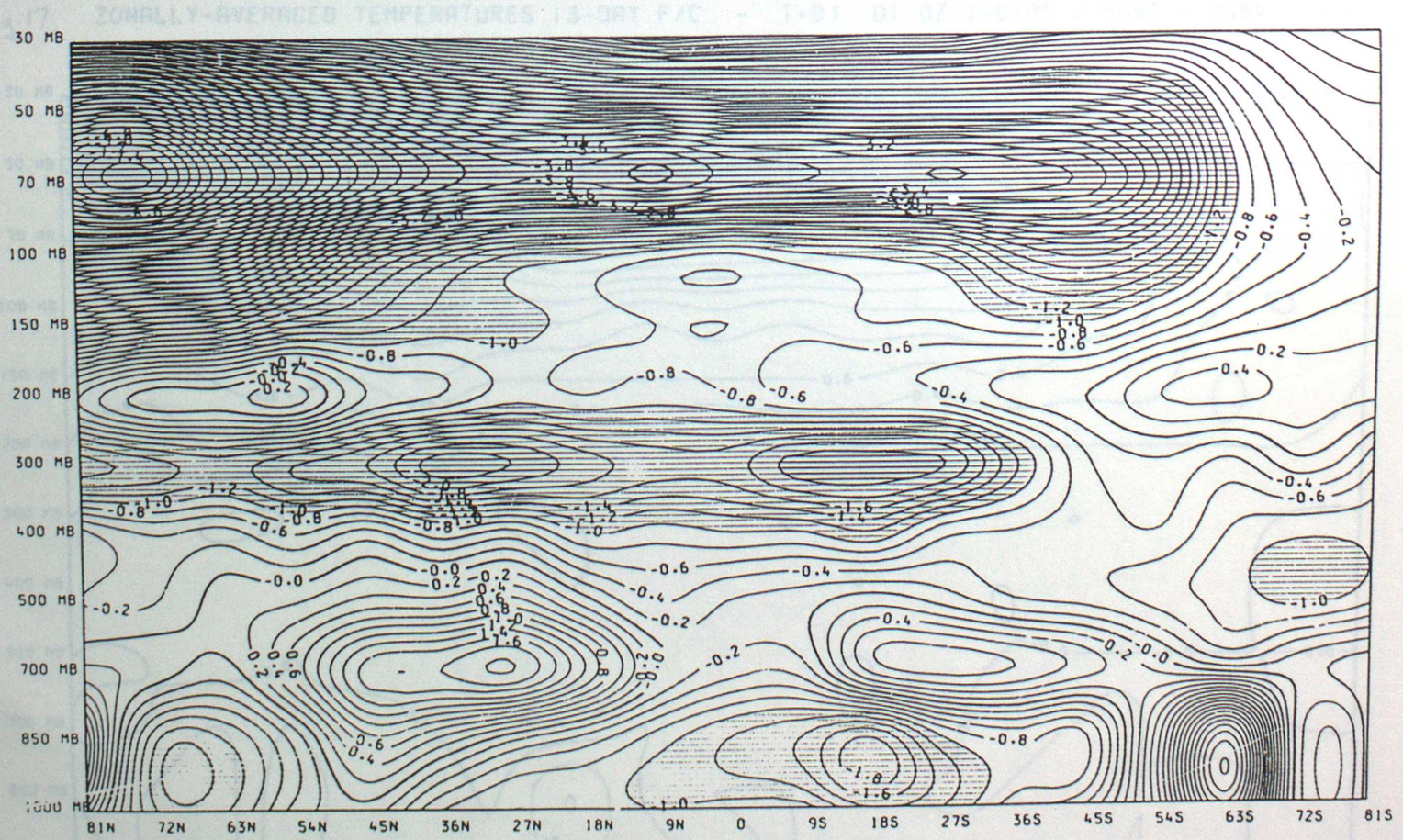

Fig.17 ZONALLY-AVERAGED TEMPERATURES (3-DAY F/C - T+0) DT 0Z 1/8/85 : RUN5 - RUN4

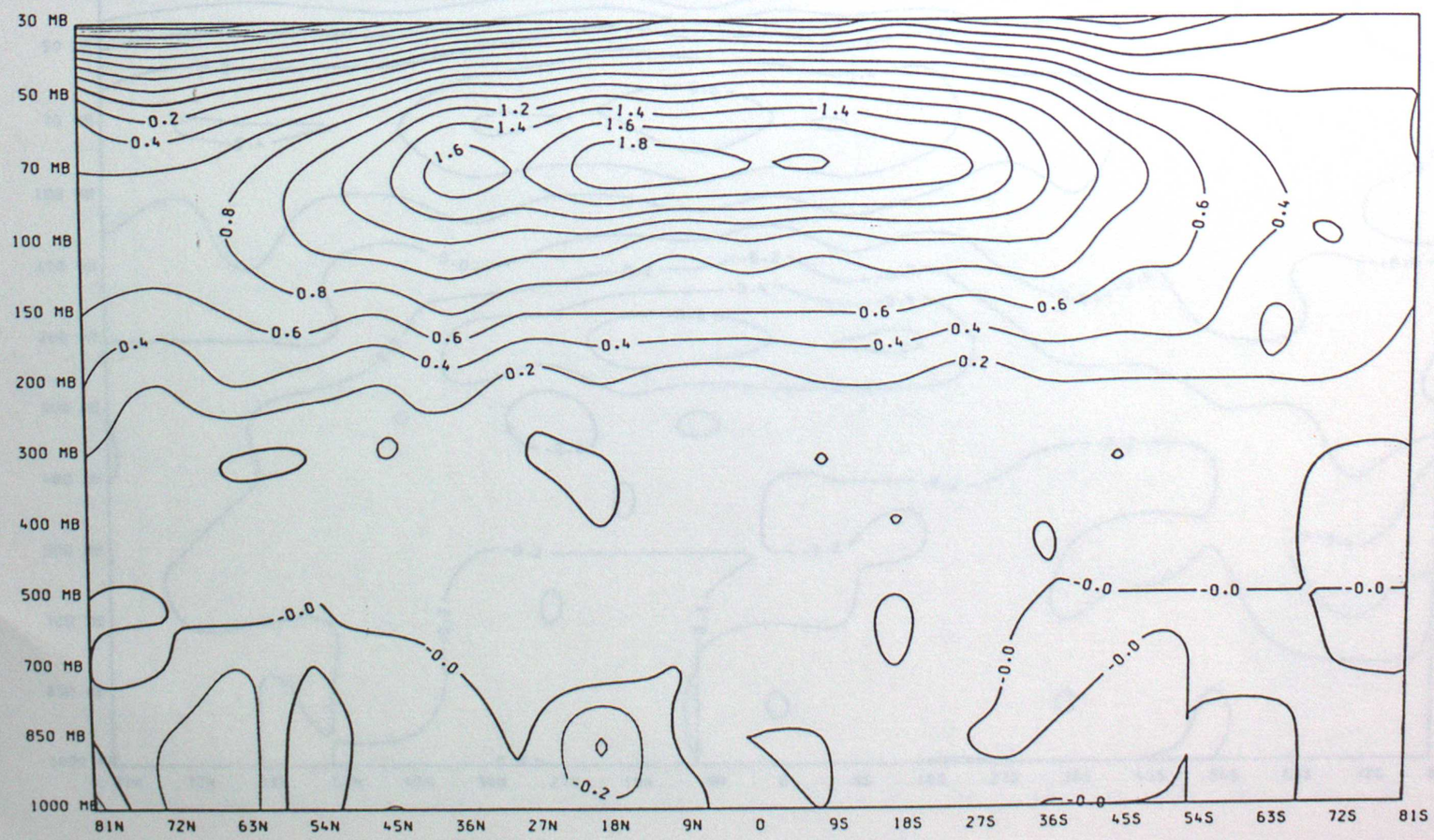

Fig. 18 ZONALLY-AVERAGED TEMPERATURES (3-DAY F/C - T+0) DT 0Z 1/8/85 : RUN7 - RUN6

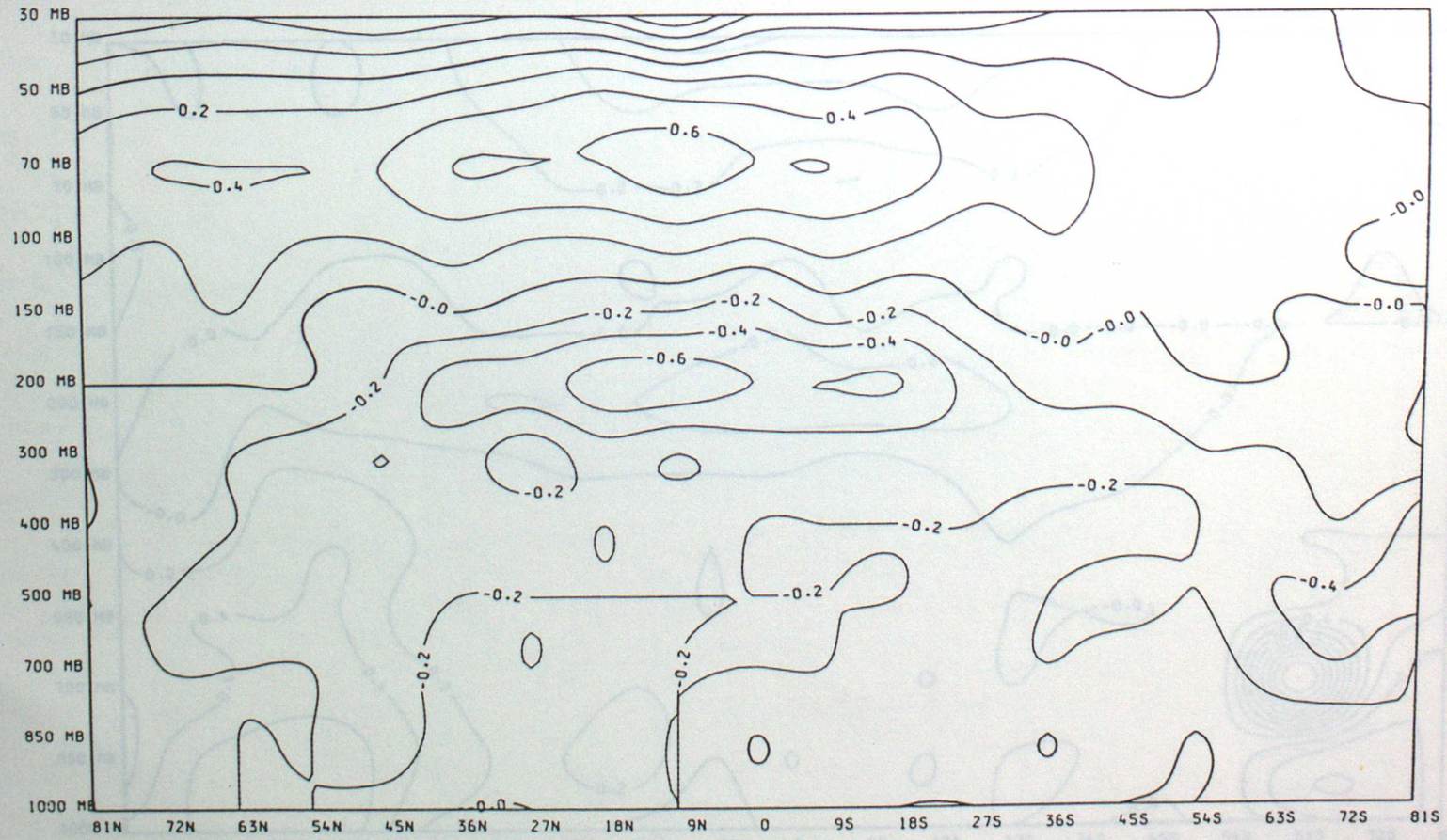

Fig. 19 ZONALLY-AVERAGED TEMPERATURES (3-DAY F/C - T+0) DT 02 1/8/85 : RUN7 - RUN8

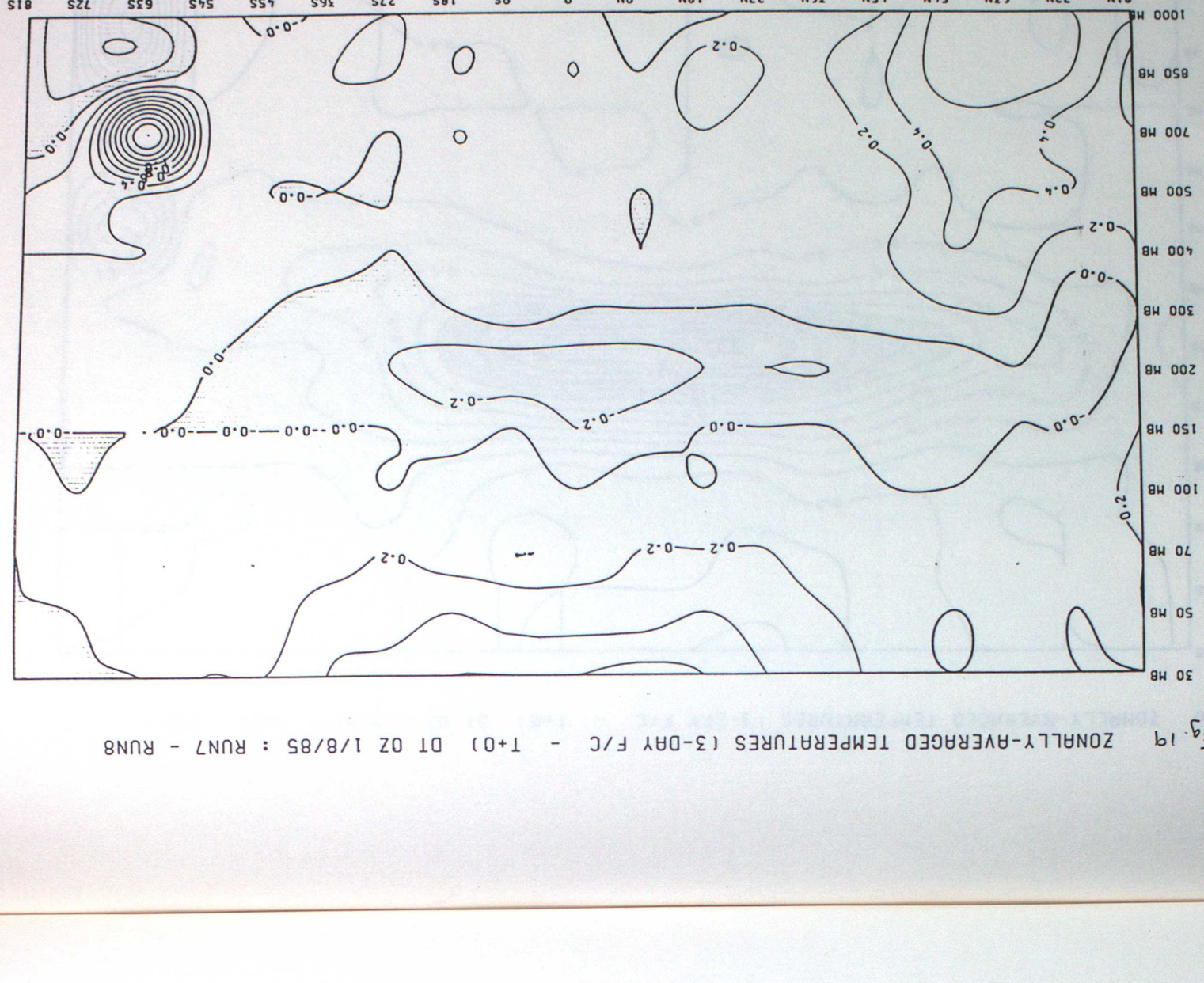

Fig. 20 ZONALLY-AVERAGED TEMPERATURES (3-DAY F/C - T+0) DT 0Z 1/8/85 : RUN9 - RUN7

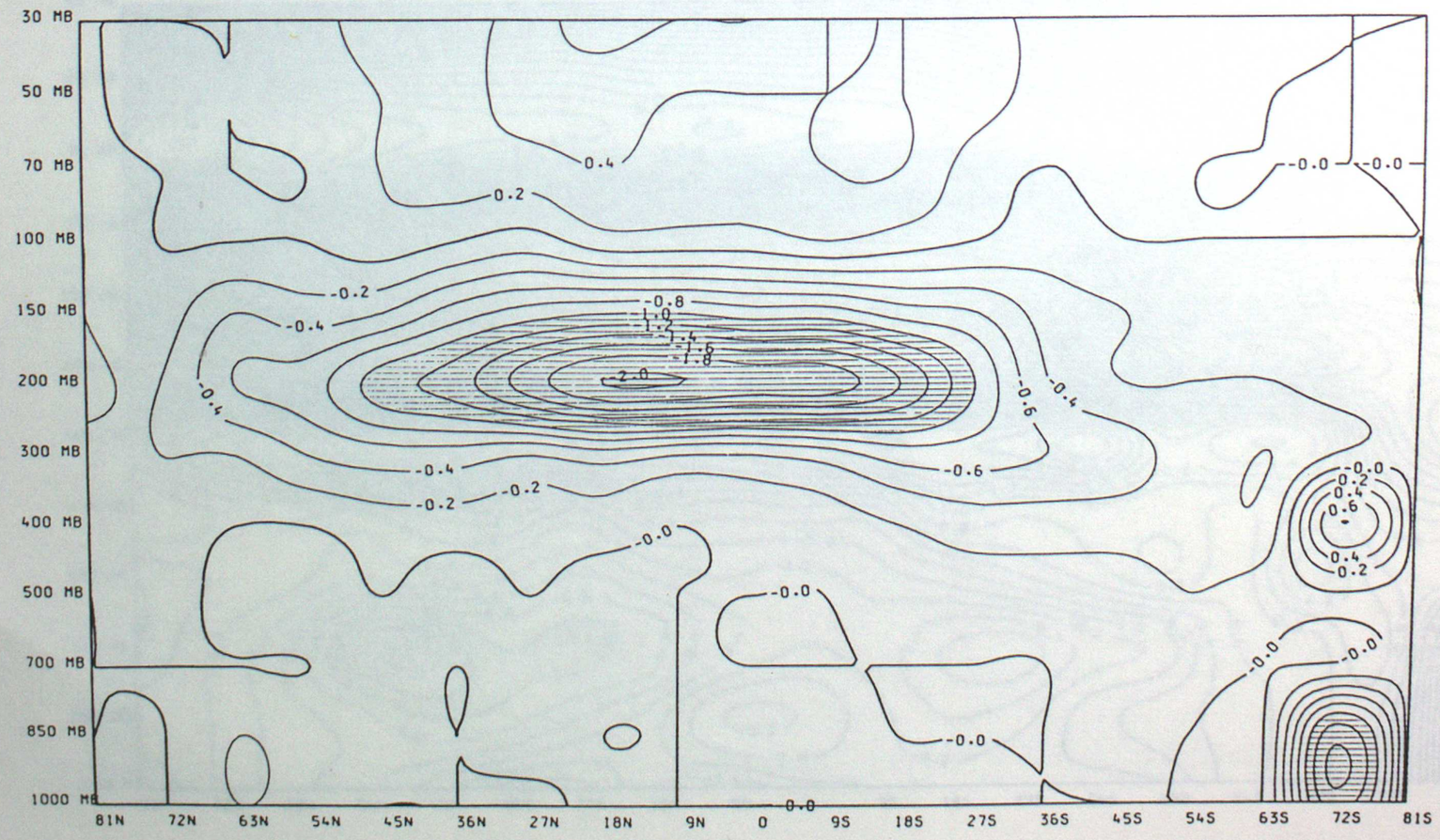

Fig 21 ZONALLY-AVERAGED TEMPERATURES (3-DAY F/C - T+0) DT 0Z 1/8/85 : RUN10- RUN26

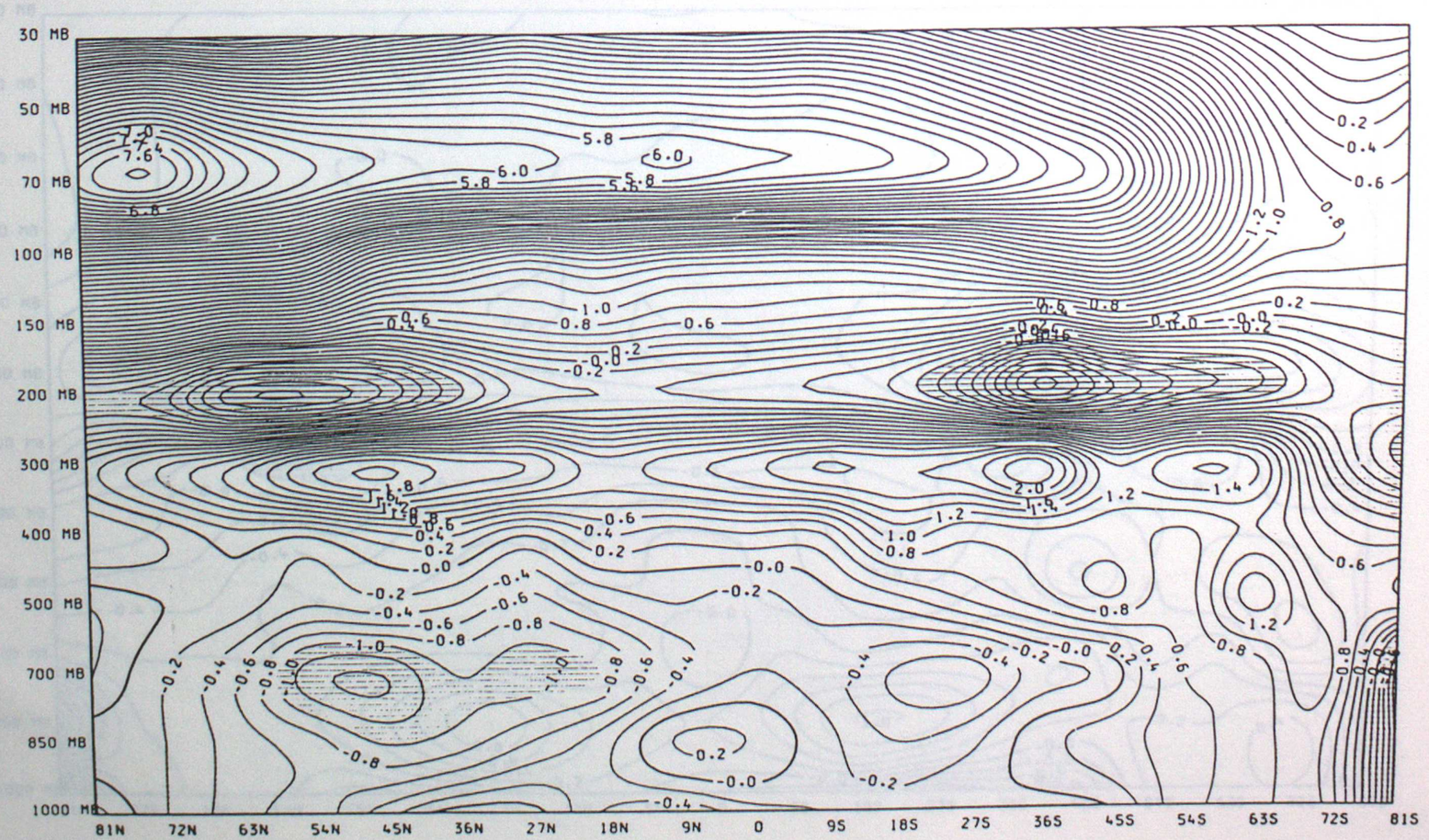

Fig.22 ZONALLY-AVERAGED TEMPERATURES (3-DAY F/C - T+0) DT OZ 1/8/85 : RUN11- RUN10

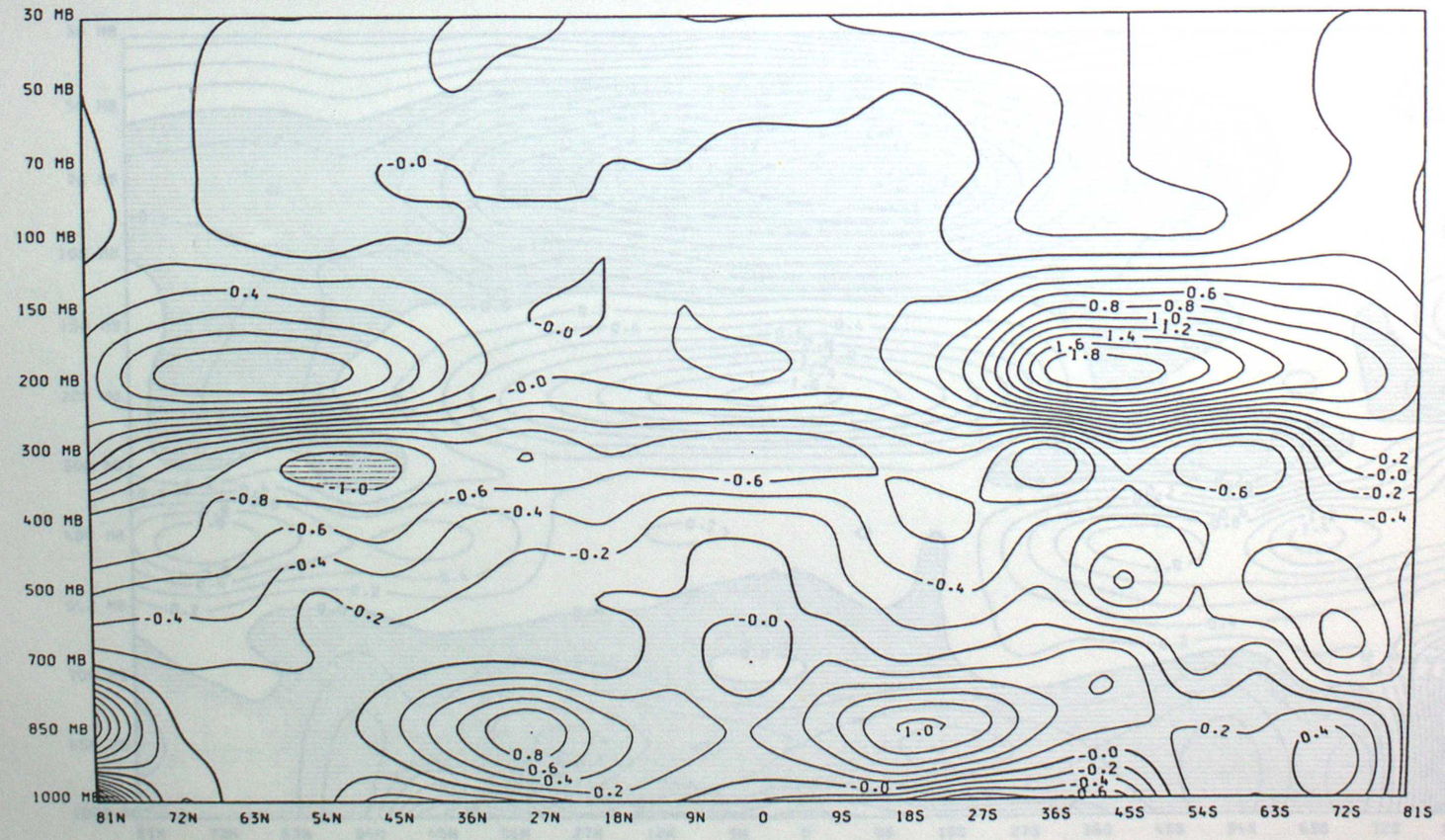

Fig. 23 ZONALLY-AVERAGED TEMPERATURES (3-DAY F/C - T+0) DT 0Z 1/8/85 : RUN13- RUN11

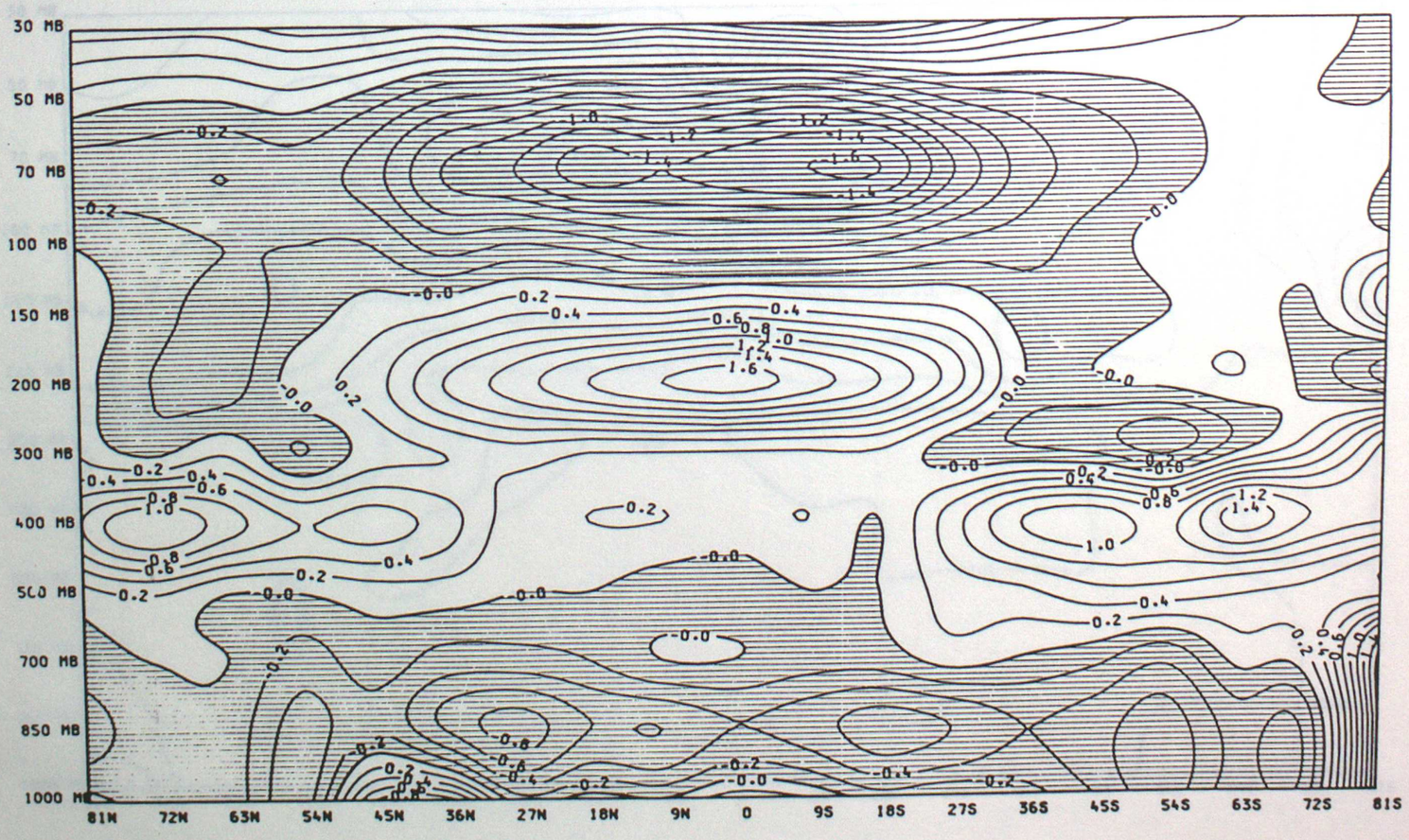

Fig.24 ZONALLY-AVERAGED TEMPERATURES (3-DAY F/C - T+0) DT OZ 1/8/85 : RUN14- RUN13

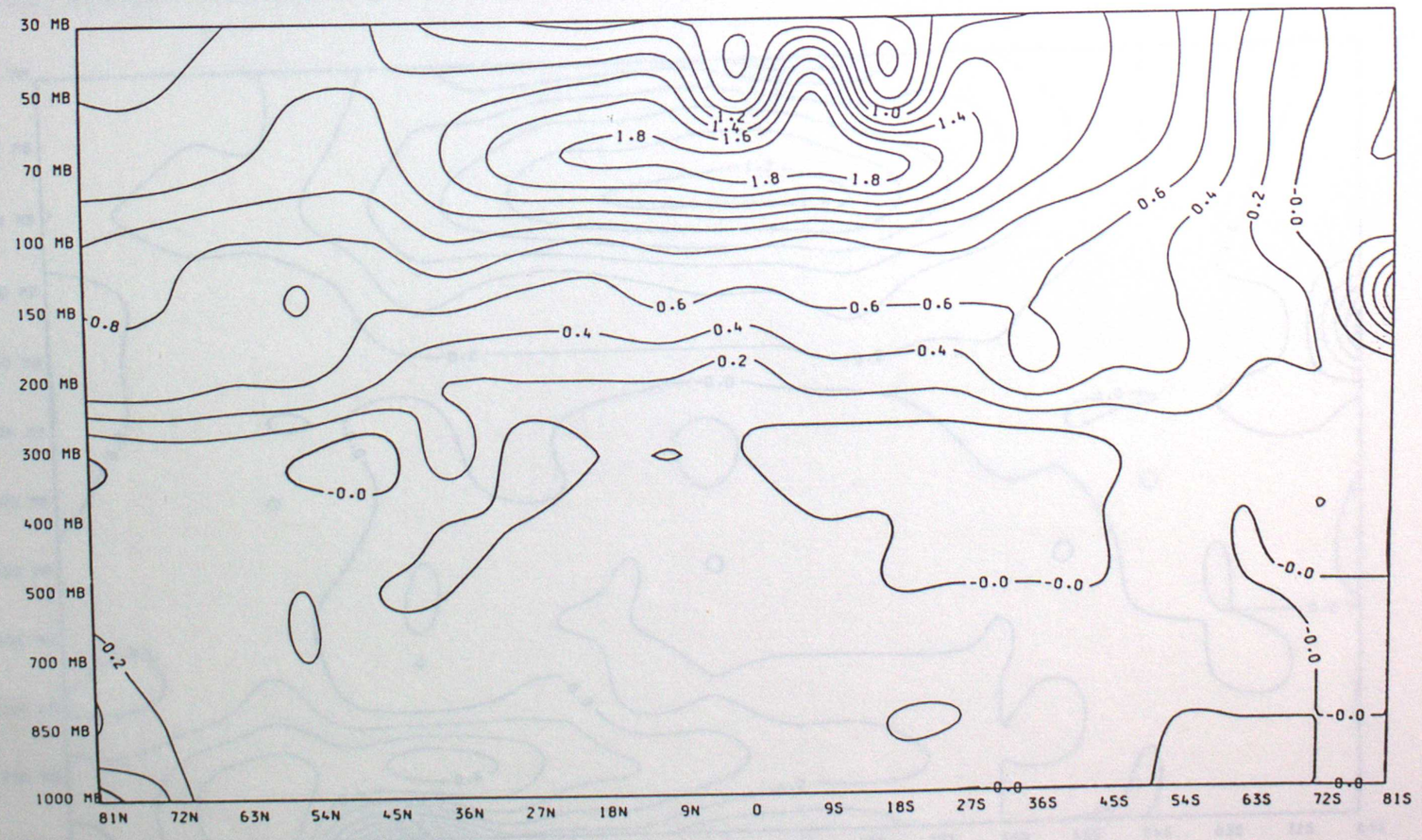

Fig.25 ZONALLY-AVERAGED TEMPERATURES (3-DAY F/C - T+0) DT 0Z 1/8/85 : RUN15- RUN13